

Modeling propagation of epidemics, social unrest and other collective behaviors

Henri Berestycki^{1,2}, Samuel Nordmann³, and Luca Rossi¹

¹Centre d'Analyse et de Mathématique Sociales, EHESS - CNRS, 54, boulevard Raspail, Paris, France

²Senior Visiting Fellow, HKUST Jockey Club Institute for Advanced Study, Hong Kong University of Science and Technology

³Department of Applied Mathematics, Tel Aviv University, Tel Aviv 6997801, Israel

April 23, 2022

Abstract

A considerable literature is devoted to the introduction and analysis of variants of the SI epidemiology models. Similar models are also proposed to describe the spread of riots and, more generally, of collective behaviors in various social contexts. The use of epidemiology models to describe such social phenomena is based on the analogy between the mechanisms of contagion and social imitation. In turn, this analogy also points to the social nature of epidemics.

This paper is concerned with a family of Reaction-Diffusion systems introduced in [17] that aims at unifying, generalizing, and enlarging the fields of application for epidemiology and collective behavior models. In this paper, we propose a modeling approach on these apparently various phenomena through the example of the dynamics of social unrest. The model involves two quantities, the level of social unrest, or, more general, activity u , and a field of social tension v , which play asymmetric roles: u is thought of as the actual observed or explicit quantity while v is an ambient, sometimes implicit field of susceptibility that modulates the growth of u .

In this article, we explore this class of model and prove several theoretical results based on the framework developed in [17], of which the present work is a companion paper. Here we place the emphasis on two subclasses of systems defined in [17]: *tension inhibiting* and *tension enhancing*. These are characterized by the fact that the unrest has respectively a negative or positive feedback on the social tension (though no monotonicity condition is assumed). In [17] we derive a *threshold* phenomenon in terms of the initial level of social tension: below a critical value, a small triggering event is quickly followed by a resumption of calm, while, above this value, it generates an eruption of social unrest spreading through space with an asymptotically constant speed. The new results we derive in the present paper concern the behavior of the solution far from the propagating edge, that is, we give a description of the new regime of the system following the initial surge of activity. We show in particular that the model can give rise to many diverse qualitative dynamics: ephemeral or limited-duration social movements – referred to as “riots” – in the tension inhibiting case, and persisting social movements – lasting upheavals – in the tension enhancing case, as well as other more complex behaviors in some mixed cases. We also investigate this model by numerical simulations that highlight the richness of this framework. We finally propose and study extensions of the model, such as spatially heterogeneous systems.

Key words: Epidemiology models · SIR model · COVID-19 · Threshold phenomenon · Modeling in social sciences · Reaction-diffusion systems · Traveling waves · Speed of propagation

Contents

1	Motivation and framework	3
2	The model	6
2.1	The dynamics of Social Unrest	6
2.2	Construction of the model	7
2.3	The model: assumptions and notations	8
2.4	Traveling waves	10
2.5	Comparison with previous models and remarks	10
3	General properties	12
3.1	Return to calm	12
3.2	Burst of Social Unrest	12
3.3	Spatial propagation	13
4	Tension Inhibiting - dynamics of a riot	13
4.1	Traveling waves	14
4.2	Large time behavior for the Cauchy problem	15
4.3	Numerical simulations	16
4.3.1	Threshold between calm and riot	16
4.3.2	Speed of propagation	16
4.3.3	Eventual level of social tension	18
5	Tension Enhancing - dynamics of a lasting upheaval	18
5.1	Traveling waves	21
5.2	Large time behavior for the Cauchy problem	21
5.3	Numerical simulations	22
5.3.1	Threshold between calm and lasting upheaval	22
5.3.2	Magnitude of the triggering event	22
5.3.3	Speed of propagation	25
6	Mixed cases	26
6.1	Double threshold: calm-riot-lasting upheaval	26
6.2	Oscillating traveling waves	28
6.3	Magnitude of the triggering event and terraces	28
7	Spatially heterogeneous models	31
7.1	Gap problem	31
7.2	Non-uniform initial social tension	31
7.3	Including geometry	34
8	Proofs	34
8.1	The tension inhibiting case	34
8.1.1	Traveling waves	34
8.1.2	Large time behavior	37
8.2	The tension enhancing case	40
9	Conclusion	42
9.1	Main findings	42
9.2	Possible extensions and perspectives	43
9.2.1	Non-local diffusion	43
9.2.2	Compartmental models	44

1 Motivation and framework

A number of large-scale phenomena, such as epidemics, riots and other collective behaviors, exhibit complex dynamics that can only be described by elaborate modeling approaches. In the current context, there is no doubt on the importance of reliable models to describe these phenomena. However, these are sometimes difficult to study empirically because of the scarcity of data and the difficulty of conducting large-scale experiments. Mathematics has a lot to offer in this field of modeling since it allow rigorous analysis, identifying the mechanisms, and testing the hypotheses through numerical experiments.

In the present circumstances, a considerable number of studies are devoted to the introduction and analysis of epidemiology models. The most widely used model in this area is undoubtedly the *SIR* compartmental model or one of the many extensions and variants. Actually the *SIR* framework is but one particular instance in the family of models introduced by Kermack and McKendrick [50]. This model features two populations: the *Susceptible*, represented by $S(t, x)$, and the *Infected*, represented by $I(t, x)$. In its simplest form (with spatial component), the model is written as the following system of two reaction-diffusion equations:

$$\begin{cases} \partial_t I - d_1 \Delta I = \beta IS - \gamma I, \\ \partial_t S - d_2 \Delta S = -\beta IS. \end{cases} \quad (1.1)$$

This model is essential in epidemic modeling, both from the point of view of theory [44–46, 58, 68, 71, 77] and applications [5, 10, 62]. However, most of the mathematical approaches available can hardly be generalized to a broader class of systems. Given the variety of extensions and variants of this model, it is a major challenge to propose a unified mathematical framework and to identify the core general properties of this class of system.

Apart from the epidemiology context, variants of the *SI* model have been proposed to account for contagion in social contexts, for example, to describe the dynamics of riots and social unrest. In their pioneering work, Burbeck et al [25] write: “*Patterns within three major riots suggest that the dynamics of the spread of riot behavior during a riot can be fruitfully compared to those operative in classical epidemics. We therefore conceptualize riots as behavioral epidemics, and apply the mathematical theory of epidemics [...].*”. This approach has been adopted in many articles dealing with the modeling of riots [15, 18, 20, 22, 27, 64, 82].

Similar ideas have also been applied to many other collective behaviors in various social contexts: the propagation of rumors [1, 4, 29, 49, 54, 65, 78, 84–86], the diffusion of a new product in a market [21, 33, 34, 36, 40, 43, 67], the propagation of ideas and scientific knowledge [3, 26, 39, 48, 51, 60], the growth of political parties [47], the propagation of memes and hashtags [37, 72, 79, 81], or extreme ideology in a society [69].

The use of epidemiology models to describe social phenomena is based on the analogy between the mechanisms of contagion, from one side, and social imitation from the other. This feature is the main driving force behind many collective behaviors, as outlined in the celebrated work of Granovetter [42], among others.

In turn, this analogy also denotes that epidemics are essentially a social phenomenon. This assertion is clearly revealed by the impacts and challenges of the current COVID-19 epidemic. As an example, we can read on the Institute of Development Studies’ website [56]: “*As the COVID-19 pandemic rages across the world, one thing is clear: this epidemic, like all others, is a social phenomenon. The dynamics of the virus, infection and immunity, not to mention on-going efforts to revise and improve clinical care, and endeavors to develop medical treatments and vaccines, are a critical part of the unfolding story. So, too, are peoples’ social responses to the disease and interactions with each other.*”

The dynamics of epidemics, riots, and other collective behaviors, although very different in nature, have a similar structure that can be described by fairly simple mechanisms. As explained by Granovetter [42], collective behaviors are situations where the inclination of an individual to join the movement depends on the intensity of the movement itself: once the movement has reached a certain size, owing to several mechanisms such as imitation or social influence, more people are prone to join it and the movement grows. It is therefore of particular importance to understand whether a small initial movement, called *triggering event*, can ignite this self-reinforcement mechanism. This involves a threshold phenomenon on an ambient level of *susceptibility*: typically, in a

context of *low susceptibility*, the *triggering event* promptly fades out, whereas, in a context of *high susceptibility*, the *triggering event* leads to a significant movement.

Our main goal in [17] and in the present article is to develop a unified mathematical framework to deal with this general setting. We aim to unify, generalize, and open new fields of application for epidemiology and collective behavior models. Let us emphasize that many articles consider non-spatial models, even though spatial diffusion often plays a key role [22, 24, 73, 82]. Our objective in [17] and here is to provide general mathematical tools to deal with these models in a unified way including spatial propagation.

In our approach, we consider the coupled dynamics of a level of *activity*, denoted by u , representing the intensity of activity (e.g. rioting activity, fraction of population having adopted a belief or a technology, etc.), and an underlying level of *susceptibility*, denoted by v , representing the ambient context. We emphasize that these two quantities play an asymmetric role: u is thought of as the actual observed or explicit quantity while v is a potential field that modulates the growth of u . From a modeling perspective, the level of activity u often represents an explicit quantity that is tractable empirically, whereas the level of susceptibility v is an implicit field. In a sense, we postulate the existence of such a field which is a lumped variable that results from several complex social interactions. Then, these two quantities interact: the field v modulates the dynamics of the activity level, and there is also a feedback mechanism whereby the level of activity influences the field of susceptibility. This is why we call this general class of systems the *activity/susceptibility* systems.

Assuming that u and v are subject to diffusion and coupled reaction, the resulting mathematical model takes the following general form:

$$\begin{cases} \partial_t u - d_1 \Delta u = \Phi(u, v) := uF(u, v), \\ \partial_t v - d_2 \Delta v = \Psi(u, v) := uG(u, v) + (v_b - v)H(u, v), \\ u(t = 0, x) = u_0(x) \geq 0 \quad ; \quad v(t = 0, x) \equiv v_b. \end{cases} \quad (1.2)$$

We aim at keeping the assumptions on the terms in the system as general as possible. In fact, the form of Φ and Ψ given in (1.2) is only suggested in this introduction to give an insight of our approach, but in the paper we actually deal with more general nonlinear terms, see Section 2.3 below.

Let us briefly justify the structural form of the above system. In a normal situation, i.e., in the absence of any exogenous event, we consider the system at equilibrium at some steady state $u \equiv 0$, $v \equiv v_b$, where the level of activity u is null and the social tension v is at its base value v_b . This is guaranteed by the special form of Φ , Ψ in (1.2). We also assume that the steady-state $(0, v_b)$ is weakly stable in a situation where $u = 0$, that is, $H(0, v) \geq 0$.

We consider that an exogenous event occurs at $t = 0$ and propose to study its effect on the system. This exogenous event is encoded in the initial condition $u_0(\cdot) \geq 0$.

As we will see, the class of systems (1.2) gives rise to many diverse qualitative behaviors. This variety is well represented by two models classes that we will investigate in more details, namely, the *tension inhibiting* case ($\Psi \leq 0$) which gives rise to an ephemeral episode of activity, and the *tension enhancing* case ($\Psi \geq 0$) which gives rise to a time-persisting episode of activity.

The class of systems (1.2) defines a paradigm which encompasses various models considered in the literature. For example, taking $\Phi(u, v) = \beta uv - \gamma u$ and $\Psi(u, v) = -\beta uv$, system (1.2) reduces to the *SI* (or *SIR*) model of epidemiology (1.1). In this context, the *Susceptible* are represented by v , and the *Infected* are represented by u : this illustrates well the role of potential field assumed by v – here the susceptibles. The term βuv accounts for the contagion from one individual to another. This term, which could be described as a law of mass action type term, is derived from the assumption that the contagion is proportional to the probability of encounter between a susceptible and an infected individual in a evenly mixed population.

A comparable mathematical model is used to describe flame propagation in a combustion process, see [9, 14, 16] and references therein. This is a typical instance of *propagation in an excitable medium*. The model features the temperature (represented by u) and the chemical fuel (represented by v). In its simplest version, assuming that the reaction is adiabatic and neglecting the hydrodynamic of the medium (for example if the medium is a solid), then the model is obtained

by taking $d_2 = 0$, $\Phi(u, v) = qF(u)v$ and $\Psi(u, v) = -F(u)v$, where $q > 0$ is a constant. The function F is given by the Arrhenius law and is typically of the type $F(u) = (u - \theta)_+$, where $\theta \in (0, 1)$ is the ignition temperature. If we include heat dissipation and assume $q = 1$, we take $\Phi(u, v) = F(u)v - \gamma u$, and we fall back to the *SIR* model with $F(u)$ instead of u .

Another example is the classical Lotka-Volterra predator-prey model, obtained by taking (overlooking various parameters) $\Phi(u, v) = u(v - \omega)$ and $\Psi(u, v) = -uv + v(1 - v)$ (with $v_b = 1$). In our context, u represents the density of *predators* and v the density of *preys*. The term $\pm uv$ represents the transfer between prey and predators (through a law of mass action type term); $-\omega u$ represents the natural death rate of predators; $v(1 - v)$ represents the natural birth rate and saturation effect (due, for instance, to the limitations of resources) in the prey population.

The class of system (1.2) encompasses other monotonic and non-monotonic systems appearing in various fields of application, such as Belousov-Zhabotinski equation for biochemical systems [76], or the Bass model in marketing [33]. See [17] for a more comprehensive discussion on the classical models that fit into the framework of (1.2).

In our paper [17], we propose a theoretical study of (1.2) in a general framework. In the present article, we discuss the significance of the results for modeling purposes. We also prove some new theoretical results concerning the long-time behavior of solutions in the *tension inhibiting* and the *tension enhancing* cases, dealing with the behaviors of solutions far from the leading edge of the front. Those results deal with both the traveling wave problem and the Cauchy problem. We accompany our analysis with several numerical simulations.

To fix ideas, we focus here on the modeling of social unrest, which is a textbook case of a propagating collective behavior. The epidemiology approach is particularly relevant in this context, as highlighted by the pioneering work of Burbeck et al. [25]. However, our approach can be envisioned to model other sociological phenomena in social sciences and population dynamics. Let us also mention that the literature on the modeling of social unrest often considers models with very particular forms, even though the quantities at stake (especially the *susceptibility*, or *social tension*) are not directly accessible from data. It thus seems important to us to develop a unified approach with minimal assumptions on the parameters.

Hence, our aim here is not to assess the validity of our model with quantitative data from the field, but rather to illustrate the richness of the framework and to discuss its qualitative relevance regarding the topic, while keeping the mathematical approach quite general.

Outline. We start with presenting, in Section 2.1, the social phenomena that we aim at describing, pointing out the basic sociological assumptions that lead, in Section 2.2, to the mathematical derivation of our model. The model and the assumptions are then stated in Sections 2.3-2.4. In Section 2.5, we discuss the existing literature on this and related topics. Section 3 is devoted to a general analysis of the model. Applying the results of [17], we enlighten a threshold phenomenon on the initial level of social tension for the ignition of a social movement. We present some estimates on the speed of propagation of the movement and comment on the interpretation of the mathematical results in terms of modeling. Next, we focus on two important classes of models: the *tension inhibiting* case (Section 4), which generates ephemeral movements of social unrest, and the *tension enhancing* case (Section 5), which gives rise to time-persisting movements of social unrest. In both cases, we present some new results about the behavior of solutions far from the leading edge of the propagating front, as well as for traveling wave solutions. These results are corroborated by numerous numerical simulations. In Section 6, we examine several mixed cases which are neither *tension inhibiting* nor *tension enhancing*, and that exhibit more complex dynamics. Section 7 deals with extensions of the model including spatial heterogeneity. Section 8 contains all the proofs of our results. Finally, Section 9 is devoted to concluding remarks and perspectives.

Remark on the numerical simulations. Numerical simulations are performed with a standard explicit Euler finite-difference scheme, with time-step $dt = 0.05$, and space-step $dx = 1$. In the caption of each figure, we give a clickable URL link and the reference to a video of the simulation available online¹.

¹Temporary address: <https://sites.google.com/view/samuelnordmann/research/modeling-social-unrest-videos>
 Definite address to be specified in the published paper.

2 The model

2.1 The dynamics of Social Unrest

In this section, we introduce our modeling assumptions on the dynamics of social unrest in society and other collective behaviors. We do not aim at discussing the sociological origins of social unrest which have given rise to a vast literature in the social sciences and continue to be studied. Instead, we propose a model built from simple ingredients to account for recurrent patterns observed in these phenomena [22, 28]. Our purpose here is to identify some possible features and mechanisms that lend themselves to mathematical analysis. Of particular importance in this respect is the dynamical unfolding and spatial spreading of social unrest.

Our approach, in the spirit of [15, 18, 20], consists of using epidemiology models to account for the coupled dynamics of social unrest and social tension. The first paper using epidemiology models to describe the mechanism of riots is due to Burbeck et al. [25]: “*A new approach to the study of large-scale urban riots has resulted in the discovery of remarkably coherent patterns in the distribution of riot events over time. Patterns within three major riots suggest that the dynamics of the spread of riot behavior during a riot can be fruitfully compared to those operative in classical epidemics. We therefore conceptualize riots as behavioral epidemics, and apply the mathematical theory of epidemics to data from the Los Angeles (1965), Detroit (1967), and Washington, D.C., (1968) riots.*”

This approach turned out to account for the dynamics of the rioting activity in a rather remarkable way. In particular, a model [22] of the class we consider here reproduces rather remarkably and precisely the dynamics and spreading of the French riots of 2005, which was triggered by the death of two young men trying to escape the police in Clichy-sous-Bois, a poor suburb of Paris. This event occurred in a context of high social tension and was the spark for the riots that spread throughout the country and lasted over three weeks.

For literature on the modeling of social unrest, riots, and related topics, we refer the reader to [15, 22, 23, 41, 42, 75] and references therein. We return in Section 2.5 to the existing literature and give a more detailed comparison between our model and several others.

We define the level of *social unrest*, abbreviated to **SU**, as the number of rioting activities or civil disobedience. We can think of **SU** as the level of illegal actions resulting from rioting, measured in some homogeneous way (e.g. number of rioting incidents reported by the police).

Our model also features a level of Social Tension, abbreviated to **ST**, accounting for the resentment of a population towards society, be it for political, economic, or for social reasons. This implicit quantity can be seen as the underlying (or potential) field of susceptibility for an individual to join a social movement.

The guiding principle of our approach rests on the hypothesis that **SU** and **ST** follow coupled dynamics.

Let us now review the most common characteristics of the dynamics of **SU** and define some vocabulary.

Even if social movements can take many different forms, it appears that they often occur as episodic *bursts*. A first simplistic classification would be to distinguish an ephemeral movement of social unrest, that we call here a “riot”, which lasts at most a couple of weeks and then fades (e.g. the London riots of 2011 [11, 28] or the French riot of 2005 [22]), from a long-duration or persisting movement of social unrest, that we call here a “lasting upheaval”, which lasts longer and can result in significant political or sociological changes (e.g. the Yellow Vest Movement [61, 80], the Arab Spring [52, 55], the Russian revolution of 1905–1907 [63], or the French Revolution. See also [6]).

However, most social protests are commonly considered to have been ignited by a single *triggering event* [31].

Accordingly, we assume that in a normal situation, the level of **SU** is null and that **ST** is at equilibrium at its base value. To account for the *triggering event*, we assume that the system is perturbed at $t = 0$.

We therefore expect that whether the *triggering event* ignites a *burst* of **SU** depends on the level of **ST**. If **ST** is high enough, a small *triggering event* triggers a *burst* of **SU**; whereas if **ST** is low, the same event is followed by a prompt *return to calm*. This threshold phenomenon was highlighted in the classical work of Granovetter [42].

These observations suggest that, in a context of low **ST**, an intrinsic mechanism of *relaxation* occurs on **SU**. The *relaxation* rate accounts for various sociological features after a burst, such as fatigue, police repression, incarceration, etc.

On the other hand, a high **ST** activates an *endogenous growth* of **SU**. In other words, if **ST** is above a threshold level, then a mechanism of self-reinforcement occurs on **SU**. This is analogous to a flame propagation (an *endogenous* growth is activated when the temperature is high enough) and pertains, more generally to “excitable media”. One can think of this *endogenous* feature as the gregarious dimension of social movements: the larger the movement, the more prone an individual is to join it [66, 70].

Naturally, this self-reinforcement mechanism can be counterbalanced by a *saturation* effect, accounting for the limited number of individuals, resources, goods to be damaged, etc.

Another important feature usually observed during movements of **SU** is the *geographical spread* [24, 82]. A striking example is the case of the 2005 riots in France [22, 74]. This phenomenon is either caused by the rioters movement as in London 2011, or by a diffusion of the riot as in France 2005. However, the role played by the geography in the dynamics of **ST** is less clear. For example, one could consider that **ST** is, or is not, affected by diffusion, or even that it is affected by a non-local diffusion (see Section 9.2.1) since information nowadays is often available instantaneously through global media.

With this vocabulary at hand, a *riot* (i.e., an ephemeral movement of social unrest) will typically be observed in a case where the *burst* of **SU** results in a *decrease* of **ST**. Once **ST** falls below a threshold value, **SU** fades and eventually stops. We call this case *tension inhibiting*. It is qualitatively comparable to the outburst of a disease, which propagates until the number of susceptible individuals falls below a certain threshold. This behavior is well captured by the famous *SI* epidemiology model, with $S = \mathbf{ST}$ and $I = \mathbf{SU}$.

On the contrary, a *lasting upheaval* (i.e., a time-persisting movement of social unrest) will typically be observed in a case where the *burst* of **SU** results in an *increases* of **ST**. In this case, the dynamics escalates towards a sustainable state of high **SU**. We call this case *tension enhancing*. From a modeling point of view, it points to a cooperative system.

These two model classes give a first good idea of the variety of behaviors generated by the model. They suggest different classes of systems: epidemiology models on the one hand and monotone systems on the other hand. Those two classes of model are studied quite separately in the literature. Our aim here is to take advantage of the unified framework of [17] to propose a single model able to encompass both behaviors.

Of course, one can also consider more complex scenarios where the feedback of **SU** on **ST** is neither positive nor negative. This situation is included in our framework and illustrated with numerous examples later on.

2.2 Construction of the model

We propose a mathematical model inspired from [15, 18, 20] to account for the dynamics of **SU** and **ST**. We let $u(t, x)$ denote the level of **SU** at given time t and position x , and let $v(t, x)$ be the level of **ST**. We consider the general form of systems of Reaction-Diffusion equations

$$\begin{cases} \partial_t u - d_1 \Delta u = \Phi(u, v), \\ \partial_t v - d_2 \Delta v = \Psi(u, v). \end{cases} \quad (2.1)$$

The diffusion terms $d_1 \Delta u(t, x)$ and $d_2 \Delta v(t, x)$ describe the influence that one location has on its *geographical neighbors*. The reaction terms Φ and Ψ model the endogenous growths and feedbacks of u and v .

The level $u = 0$ represents the absence of social unrest, or activity. The value v_b stands for the *base value* of the social tension in the normal (quiet) regime. We assume that the system is at equilibrium in the quiet regime, that is, $(u \equiv 0, v \equiv v_b)$ is a steady state for (2.1) ($\Phi(0, v_b) = \Psi(0, v_b) = 0$). For example, we can choose, as in (1.2),

$$\Phi(u, v) = uF(u, v) \quad ; \quad \Psi(u, v) = uG(u, v) + (v_b - v)H(u, v). \quad (2.2)$$

We further assume that v_b is a weakly stable state for the second equation when $u \equiv 0$, i.e., $\Psi(0, v) \geq 0$ if $v \leq v_b$ and $\Psi(0, v) \leq 0$ if $v \geq v_b$. Under the particular form (2.2), it amounts to saying that $H(0, \cdot) \geq 0$ (which is the case of the *SI* system, where $H \equiv 0$).

We then introduce a *triggering event*. This corresponds to a small perturbation of the steady-state ($u = 0, v = v_b$) and is encoded in the initial condition. For simplicity, we suppose that the initial perturbation only occurs on the u component, that is, we take $v_0(\cdot) \equiv v_b$. We study the case of more general initial conditions v_0 in [17].

We choose the term Φ in the first equation of (2.1) to be of the form

$$\Phi(u, v) := u[r(v)f(u) - \omega].$$

The term $f(u)$ represents the *endogenous* factor (or self-reinforcement/saturation mechanism). We take f nonincreasing (to account for a saturation effect) and positive at $u = 0$; for example, $f(u) = 1 - u$ or $f(u) = 1$.

The parameter $\omega > 0$ is the natural rate of *relaxation* of SU in absence of self-reinforcement.

The endogenous factor is regulated by $r(v)$, which models the role of *activator* played by ST. We choose $r(\cdot)$ to be nonnegative and increasing. We can think of this term as an on-off switch of the endogenous growth. For example, $r(\cdot)$ can be linear $r(v) = v$, or take the form of a sigmoid

$$r(v) = \frac{1}{1 + e^{(\alpha - v)\beta}},$$

where, $\alpha \geq 0$ is a threshold value while $\beta > 0$ measures the stiffness of the transition between the relaxed state and the excited state (the case $\beta = +\infty$ corresponds to $r(v) := \mathbb{1}_{v > \alpha}$).

Let us emphasize that most of our theoretical results can be adapted to a more general function Φ , see [17]. We choose this particular form for convenience and to make clearer the interpretation in terms of modeling.

Let us now describe the reaction term Ψ in the second equation of (2.1). For the sake of clarity, we want to normalize v such that it ranges in $(0, 1)$; thus we will assume that $v_0 \in (0, 1)$, $\Psi(u, 0) \geq 0$ and $\Psi(u, 1) \leq 0$. We devote a particular attention to the following two classes of models. Each case illustrates a typical qualitative behavior.

1. *The tension inhibiting case:* $\Psi(u, v) < 0$ for $u > 0, v \in (0, 1)$. In this case, a *burst* of u causes a *decrease* of v . We expect this case to give rise to an ephemeral riot and to behave comparably to the *SI* epidemiology model, in which

$$\Psi(u, v) = -\beta uv,$$

with $\beta > 0$.

2. *The tension enhancing case:* $\Psi(u, v) > 0$ for $u > 0, v \in (0, 1)$. In this case, a *burst* of u causes an *increase* of v . We expect this case to give rise to a lasting upheaval and to behave comparably to a cooperative system (although we do not assume that Ψ is monotonic). As an example, we can take

$$\Psi(u, v) = uv(1 - v).$$

2.3 The model: assumptions and notations

We consider $u(t, x)$, which stands for the level of social unrest at time $t \geq 0$ and location $x \in \mathbb{R}^n$, and $v(t, x)$, which stands for the level of social tension, solution of

$$\begin{cases} \partial_t u - d_1 \Delta u = \Phi(u, v) := u[r(v)f(u) - \omega], \\ \partial_t v - d_2 \Delta v = \Psi(u, v), \\ u(0, x) := u_0(x), \quad v(0, x) := v_0(x). \end{cases} \quad (2.3)$$

Here are our standing assumptions, that will be understood throughout the paper:

- a) $d_1 > 0, d_2 \geq 0, \omega > 0$.
- b) $f(u)$ is smooth and nonincreasing on $[0, +\infty)$, with $f(0) > 0$; for example, $f(u) = 1$ or $f(u) = 1 - u$.
- c) $r(v)$ is smooth, nonnegative and increasing on $(0, 1)$; for example, $r(v) = v$.

d) $r(0) < \frac{\omega}{f(0)} < r(1)$, and we define

$$v_\star := r^{-1} \left(\frac{\omega}{f(0)} \right) \in (0, 1). \quad (2.4)$$

e) $\Psi(0, \cdot)$ has a (weakly) stable zero $v_b \in (0, 1)$, i.e.,

$$\Psi(0, v) \geq 0, \quad \forall v \in (0, v_b) \quad ; \quad \Psi(0, v) \leq 0, \quad \forall v \in (v_b, 1); \quad (2.5)$$

for example, $\Psi(0, \cdot) \equiv 0$.

f) $\Psi(u, v)$ is smooth and satisfies the saturation conditions at $v = 0, 1$

$$\Psi(u, 0) \geq 0 \quad \text{and} \quad \Psi(u, 1) \leq 0 \quad \forall u \geq 0. \quad (2.6)$$

g) $u_0(x) \geq 0$ is bounded and $v_0 \equiv v_b$, where v_b is a constant defined in assumption (2.5).

Our set of assumptions covers many diverse systems, which may be highly non-monotone and exhibit quite different qualitative behaviors, as illustrated in the sequel. We give in [17] a more detailed discussion on the link between this system and several others, such as the *SI* (or *SIR*) epidemiology model or predator-prey systems.

The particular form of Φ and the monotonicity assumptions on f and r are not strictly necessary but allow to simplify the presentation. Also, most of our result extend to the case where $v_0 - v_b$ is compactly supported. Since, here, we assume $v_0 \equiv v_b$, we shall write indifferently v_0 or v_b . We refer the reader to [17] for results in a more general framework.

If one assumes that $\Psi(0, \cdot) \equiv 0$, then (2.5) is automatically satisfied and thus any $v_b \in (0, 1)$ is suitable for our set of assumptions.

The following property is an immediate consequence of our assumptions.

Lemma 2.1. *Any solution of (2.3) satisfies*

$$u(t, x) > 0 \quad \text{and} \quad 0 < v(t, x) < 1, \quad \forall t > 0, x \in \mathbb{R}^n.$$

Proof. Recall that $u_0 \geq 0$ and $v_0 \in (0, 1)$. For the range of v , we notice that in view of (2.6), v satisfies the inequalities

$$\partial_t v - d_2 \Delta v - (\Psi(u, v) - \Psi(u, 0)) = \Psi(u, 0) \geq 0,$$

and

$$\partial_t (1 - v) - d_2 \Delta (1 - v) - (\Psi(u, 1) - \Psi(u, v)) = -\Psi(u, 1) \geq 0.$$

This implies that $v(t, x)$ has range in $(0, 1)$, thanks to the parabolic strong comparison principle if $d_2 > 0$, or simple ODE considerations if $d_2 = 0$. Analogously, since the constant 0 is a solution of the first equation in (2.3), we have that $u(t, x) > 0$ for $t > 0, x \in \mathbb{R}^n$. \square

The quantity v_\star defined by (2.4) coincides with the value of v where $\partial_u \Phi(0, v)$ changes sign, i.e.,

$$v_\star := \sup \left\{ v \in (0, 1) : r(v) \leq \frac{\omega}{f(0)} \right\} = \sup \{ v \in (0, 1) : \partial_u \Phi(0, v) \leq 0 \}.$$

We will see in the sequel that v_\star is the threshold value on $v_0 \equiv v_b$ which determines the regime of dynamics:

- if $v_b < v_\star$, a small *triggering event* is followed by a *return to calm*,
- if $v_b > v_\star$, a small *triggering event* ignites a *burst* of social unrest. This is akin to the *Hair-trigger* effect in KPP equations.

The assumption (2.4) allows us to cover both possibilities of a *burst* or a *return to calm* depending on the choice of $v_b \in (0, 1)$.

The above dichotomy is readily revealed by the analysis of the constant steady states of (2.3). Namely, consider the scalar equation (with unknown u)

$$\Phi(u, v_b) := u[r(v_b)f(u) - \omega] = 0, \quad u \geq 0, \quad (2.7)$$

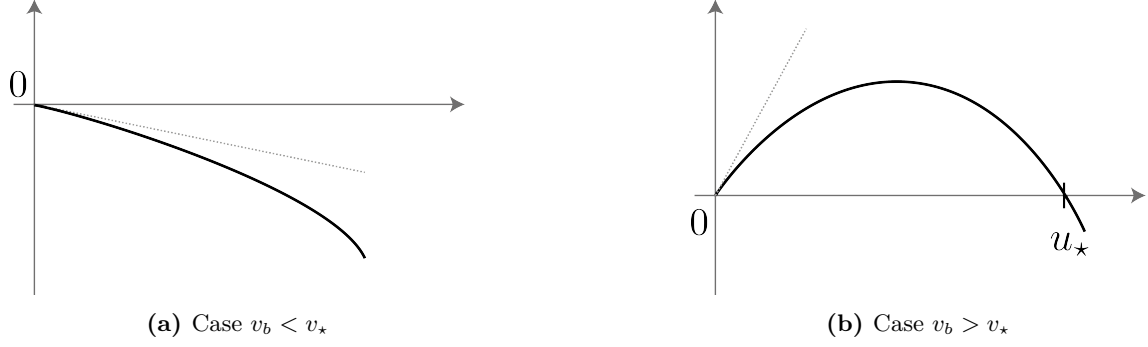


Figure 1: Graph of $u \mapsto \Phi(u, v_b)$ depending on the base level of tension v_b . The dashed line represents the slope at the origin (i.e. K_b).

under the assumption that f is strictly decreasing and $f(1) = 0$. Call

$$K_b := \partial_u \Phi(0, v_b) = r(v_b)f(0) - \omega. \quad (2.8)$$

Note that, since $r(\cdot)$ is increasing, the sign of K_b coincides with that of $v_b - v_*$. We have the following dichotomy:

- If $v_b < v_*$, then $K_b < 0$, and (2.7) has exactly one solution $u = 0$ (stable). See Figure 1a.
- If $v_b > v_*$, then $K_b > 0$, and (2.7) has exactly two solutions, $u = 0$ (unstable) and $u = u_*(v_b)$ (stable), defined by

$$u_*(v) := f^{-1} \left(\frac{\omega}{r(v)} \right). \quad (2.9)$$

See Figure 1b. Note that $v \mapsto u_*(v)$ is continuous increasing and that $u_*(v) \searrow 0$ as $v \searrow v_*$. For example, if $f(u) = 1 - u$ and $r(v) = v$, then $v_* = \omega$ and $u_*(v) := 1 - \frac{\omega}{v}$.

2.4 Traveling waves

It is reasonable to expect that, when a burst of social unrest occurs, the solution of (2.3) converges to a *traveling wave*, that is, an identical profile moving at a constant speed. Although we do not prove such a result, we corroborate it with numerical evidence in the sequel. It is thus interesting to study the existence, non-existence, and the shape of traveling waves.

A traveling wave is defined as a solution of (2.3) of the form $u(t, x) = U(x \cdot e + ct)$, $v(t, x) = V(x \cdot e + ct)$, with $c > 0$, $e \in \mathbb{S}^{n-1}$ and prescribed values at $-\infty$. The profiles $U(\xi)$ and $V(\xi)$ thus satisfy the elliptic problem

$$\begin{cases} -d_1 U'' + cU' = \Phi(U, V) := U[r(V)f(U) - \omega], \\ -d_2 V'' + cV' = \Psi(U, V), \\ c > 0 \quad ; \quad U > 0 \text{ is bounded} \quad ; \quad 0 < V < 1. \end{cases} \quad (2.10)$$

We complete it with the *semi-boundary conditions* at $-\infty$

$$\begin{cases} U(-\infty) = 0, \\ V(-\infty) = v_b. \end{cases} \quad (2.11)$$

The term *semi-boundary conditions* comes from the fact that we do not impose a prescribed value at $+\infty$. The traveling waves under consideration might not be unique and may take many diverse forms, such as monotone waves or bumps. This will be illustrated in the following sections.

2.5 Comparison with previous models and remarks

Our model is directly inspired by a series of papers [15, 18, 20] which introduce a system of Reaction-Diffusion equation, comparable to (2.3), to model the dynamics of riots. As before, the quantity $u(t, x)$, depending on time $t \geq 0$ and location $x \in \mathbb{R}^n$, represents the level of social unrest, and

$v(t, x)$ represents the level of social tension. In most cases, the model reduces to the following system

$$\begin{cases} \partial_t u = d\Delta u + ur(v)f(u) - \omega(u - u_b(x)), \\ \partial_t v = d\Delta v + S(t, x) - \theta \left(\frac{1}{(1+u)^p} v - v_b(x) \right). \end{cases} \quad (2.12)$$

This model has been first introduced [15].

Let us describe the model (2.12) and discuss the main differences with our model (2.3). The parameters $r(\cdot)$, $f(\cdot)$ and ω are the same as described in the previous section. The quantity $\theta > 0$ stands for the natural relaxation rate on the level of social tension to the base rate v_b in absence of any rioting activity.

The function $u_b(x)$ stands for the low recurrent rioting activity in the absence of any unusual factors. Accordingly, $v_b(x)$ denotes the base level of social tension in absence of any rioting activity. Our model (2.3) corresponds to the case where u_b and v_b are constant (using the change of variable $\tilde{u} := u - u_b$).

With non-constant $u_b(x)$ and $v_b(x)$, the model (2.12) is spatially heterogenous. On the contrary, our model (2.3) is spatially homogeneous. The non-homogeneous setting is however an interesting perspective and is discussed in Section 7.

The parameter $p \in \mathbb{R}$ models the feedback of u on v . If $p > 0$, then a *burst* of u will *slow down* the relaxation of v ; if $p < 0$, then a *burst* of u will *speed up* the relaxation of v . If $p = 0$, the system is decoupled. In [18, 20], the cases $p < 0$ and $p > 0$ are called respectively *tension enhancing* and *tension inhibiting*, however it does not correspond to what we call *tension enhancing* and *tension inhibiting* in the present work. Let us be more precise. Assume for simplicity that $v_b \equiv 0$ and $S \equiv 0$. In (2.12), the cases $p > 0$ and $p < 0$ model respectively a negative and a positive feedback of u on v . However, the fact that the term $-\theta \frac{1}{(1+u)^p} v$ is negative results in the fact that $t \mapsto v(t, x)$ is decreasing and decays to 0, regardless of the sign of p . This implies that any burst of social unrest eventually vanishes. The behavior observed in (2.12) in both cases $p > 0$ and $p < 0$ is well captured by what we call *tension inhibiting* in the present work (Section 4). System (2.12) does not model a situation where a burst of social unrest results in an increase of the social tension. Yet, this case is reasonable from the modeling perspective and allows to account for time-persisting movement of social unrest (see Section 5).

In [15, 18, 20], the source term $S(t, x)$ accounts for *exogenous events*. In the present paper, we consider that a single exogenous event occurs at time $t = 0$ and encode it in the initial conditions.

In [20], the authors focus on the effect of a restriction of information, which is modeled by substituting the KPP term $uf(u)$ with the combustion term $(u - \alpha)_+ f(u)$, $\alpha \in (0, 1)$, where the subscript $+$ denotes the positive part. The paper [18] considers (2.12) without space (i.e. $d = 0$) and studies the dynamics of the system for a periodic source term

$$S(t) := A \sum_{i \geq 0} \delta_{t=iT}.$$

We also mention [82] in which a numerical analysis is conducted to investigate the influence of the parameters on the shape and speed of traveling waves. The article [19] also proposes a model comparable to (2.12) for criminal activity.

A recent work [64] proposes another model to account for the dynamics of social unrest quite different in spirit from the model we discuss here. In this work, $u(t, x)$ represents the number of individuals that take part in the social movement. It is assumed to satisfy the equation

$$\partial_t u - d_1 \partial_{xx}^2 u = \varepsilon_0 + \varepsilon u + \frac{au^2}{h^2 + u^2} - m(t, x)u, \quad (2.13)$$

where ε_0 , ε , a and h are positive constants. The term $\varepsilon_0 + \varepsilon u$ stands for the rate at which people are willing to join the social movement. The nonlinear term $\frac{au^2}{h^2 + u^2}$ accounts for a saturation effect. The quantity $m(t, x)$ represents the rate at which individuals exit the movement. It can be thought as a field of *non-susceptibility*, and is somehow opposite to v in our model. It is assumed in [64] that m is either constant, or given by the explicit formula

$$m(t) = m_1 + (m_0 - m_1)e^{-bt},$$

or by the equation

$$\partial_t m - d_2 \partial_{xx}^2 m = \beta u \quad ; \quad m(t = 0, x) = m_0.$$

Let us emphasize that, for some range of parameters, the equation on u is of the bistable type. For example, if $\varepsilon_0 = 0$ and m is a constant lying in the interval $(\varepsilon, \varepsilon + \frac{a}{2h})$, then equation (2.13) admits three constant steady states (two of them are stable and the third one is unstable). This differs from our model in which u satisfies a monostable equation.

Finally, we mention that many other mathematical approaches have been taken to model the dynamics of riots, protests and social unrest, such as individual-based models [32, 35], cost/benefits analysis [28], or diffusion on networks [83]. The pioneering paper using epidemiology models for riots is due to Burbeck et al. [25].

3 General properties

In this section, we state general properties on the system (2.3) under the assumptions presented in Section 2.3. These results are established in [17]. Here, we apply the results of [17] in our context and discuss the implications in terms of modeling. In particular, we highlight a threshold phenomenon on the initial level of social tension for a small *triggering event* to ignite a movement of social unrest.

3.1 Return to calm

First, let us observe that in a context of low social tension, a *small triggering event* is followed by a *return to calm*. Mathematically speaking, if $v_b < v_*$, with v_* defined in (2.4), the steady state ($u = 0, v = v_b$) is stable with respect to a small perturbation on u . Indeed, from [17, Theorem 1], if $d_2 > 0$ and $v_0 \equiv v_b < v_*$, then any solution with u_0 sufficiently small and compactly supported, satisfies

$$\lim_{t \rightarrow +\infty} (u(t, x), v(t, x)) = (0, v_b), \quad \text{uniformly in } x \in \mathbb{R}^n. \quad (3.1)$$

This has two implications from the modeling point of view. First, it means that a *triggering event* with small intensity has no effect in the long run. Furthermore, since the convergence is uniform in space, it means that a *localized triggering event* has a localized effect.

Under the same conditions, but with $d_2 = 0$, and $u_0 < \varepsilon$ small but not necessarily compactly supported, there holds that

$$\begin{cases} \lim_{t \rightarrow +\infty} u(t, x) = 0, & \text{uniformly in } x \in \mathbb{R}^n, \\ \sup_{x \in \mathbb{R}^n} |v(t, x) - v_b| \leq C\varepsilon, & \forall t \geq 0, \end{cases}$$

for some constant C independent of u_0 and ε . This expresses the fact that a *triggering event with small intensity*, even if spread out, will have a small effect on the system.

We point out that, in the *tension inhibiting case* (c.f. assumption (4.1) below), the above results hold true for u_0 not necessarily small, see [17, Theorem 6].

3.2 Burst of Social Unrest

In contrast with the above *return to calm*, when the initial level of social tension is sufficiently large, an arbitrarily small *triggering event* ignites a movement of social unrest. This feature is usually called a *Hair-trigger effect*.

In other words, if $v_0 \equiv v_b > v_*$ defined by (2.4), the steady state $(0, v_b)$ is unstable. Namely, from [17, Theorem 1], we know that for any $x_0 \in \mathbb{R}^n$ and $r > 0$, there holds that

$$\limsup_{t \rightarrow +\infty} \left(u(t, x_0) + \sup_{x \in B_r(x_0)} |v(t, x) - v_b| \right) > 0. \quad (3.2)$$

This means that even a small event is sufficient to trigger a *burst* of social unrest, which will drive the system away from the initial condition. This can be put in contrast with the scenario when $v_0 \equiv v_b < v_*$ for which (3.1) occurs.

Aside from property (3.2), the asymptotic behavior of the solution can be diverse, as revealed by numerical simulations presented later on in this paper. Nevertheless, we are able to detail the picture for two important and general classes of systems: the *tension inhibiting* systems or *tension enhancing* systems, see Sections 4 and 5 respectively.

3.3 Spatial propagation

Next, we investigate the long-range effect and the geographical spreading of a *burst*. When $v_0 \equiv v_b > v_*$ given by (2.4), we define

$$c_b := 2\sqrt{d_1(r(v_b)f(0) - \omega)}, \quad c_1 := 2\sqrt{d_1(r(1)f(0) - \omega)}. \quad (3.3)$$

Note that $c_b < c_1$ because $r(\cdot)$ is increasing and $v_b < 1$. Then [17, Theorem 2] states that, for any $x_0 \in \mathbb{R}^n$, $r > 0$ and any direction $e \in \mathbb{S}^{n-1}$, the following hold:

$$\forall c \in (0, c_b), \quad \limsup_{t \rightarrow +\infty} \left(u(t, x_0 + cte) + \sup_{x \in B_r(x_0)} |v(t, x + cte) - v_b| \right) > 0, \quad (3.4)$$

$$\forall c > c_1, \quad \lim_{t \rightarrow +\infty} \left(\sup_{|x| \geq ct} |(u(t, x), v(t, x)) - (0, v_b)| \right) = 0. \quad (3.5)$$

From the modeling point of view, it means that a localized triggering event leads to a movement of social unrest that propagates through space. More precisely, an observer moving at a speed c eventually outruns the propagation if $c > c_1$, whereas, if $c < c_b$, he will face situations away from the quiet state $(0, v_b)$.

Properties (3.4)-(3.5) do not allow us to assert the existence of an *asymptotic speed of propagation*, as usually intended, because of the gap between c_b and c_1 and also of the fact that we only have a “lim sup” in (3.4). The gap between c_b and c_1 is filled in the inhibiting case, because we show in [17] that in such case property (3.5) holds with c_1 replaced by c_b . That is, in this case, c_b is the asymptotic speed of propagation. The numerical simulation in Section 5.3.3 shows that in the general case the *asymptotic speed of propagation* may be different from both c_b and c_1 . We also show in [17] that, in the enhancing case, we can replace the “lim sup” with a “lim inf” in (3.4). This means that an observer moving at speed $c < c_b$ faces an *excited scenario* for all sufficiently large times.

4 Tension Inhibiting - dynamics of a riot

We consider our main equation (2.3). The *tension inhibiting* structure relies on following negativity assumptions on Ψ :

$$\begin{cases} \Psi(u, v) < 0 & \text{for all } u > 0, v \in (0, 1), \\ \limsup_{u \rightarrow +\infty} \frac{\Psi(u, v)}{u} < 0 & \text{locally uniformly in } v \in (0, 1]. \end{cases} \quad (4.1)$$

In particular, in view of the saturation assumption (2.6), there holds that $\Psi(u, 0) = 0$ for all $u \geq 0$.

Assumptions (4.1) essentially mean that u has a negative feedback on v (however, we do not assume any monotonicity on $u \mapsto \Psi(u, v)$ as in the *SI* model (1.1)). As a direct consequence of this assumption and the parabolic comparison principle (or ODE considerations if $d_2 = 0$), we have that

$$v(t, x) < v_0 = v_b, \quad \forall t > 0, x \in \mathbb{R}^n.$$

A typical example of a *tension inhibiting* system is the celebrate *SI* epidemiology model (1.1). This system enters the general class (2.3) by taking $r(v) = v$, $f(u) = u$, and $\Psi(u, v) = -uv$ in (2.3). Note that the *SI* model is inhibiting for any $v_b \in (0, 1)$.

As we will see, the *tension inhibiting* case typically grasps the dynamics of a limited-duration movement of social unrest, that we call a *riot*. A good heuristics of the behavior of the model is given by a formal analysis of the underlying *ODE* system. Consider a constant initial datum u_0 , hence the solutions $u(t, x)$ and $v(t, x)$ of (2.3) do not depend on x . In this case, we easily see that if the initial level of social tension v_b is above the threshold v_* then the system features a *Hair-trigger effect*, that is, any *triggering event* (i.e., $u_0 > 0$) ignites a movement of social unrest. Then, from assumption (4.1), the level of social tension decreases, until it goes below than the threshold value v_* . At this point, the level of social unrest begins to fade and eventually goes to 0, while the level of social tension converges to some final state smaller than the initial one.

The same qualitative behavior is observed in the context of epidemiology, where v represents the number of susceptible and the number of infected. When an epidemic spreads out, the susceptible population decreases until it goes below a threshold value, after what the infection dies out.

The goal of this section is to recover, at least partially, the above properties for the PDE general system (2.3). We begin with the study of traveling waves, next we present partial results for solutions of the Cauchy problem. We conclude this section with detailed numerical simulations.

4.1 Traveling waves

Let us first reclaim from [17] the existence and non-existence results for traveling waves, i.e., solutions to (2.10)-(2.11). Recalling that the sign of $v_b - v_*$ (from definition (2.4)) coincides with the one of K_b (from (2.8)), [17, Theorem 8] implies that the following hold under the inhibiting assumption (4.1):

- if $v_b < v_*$, there exists no traveling wave;
- if $v_b > v_*$, there exists no traveling wave with speed $c < c_b$ and there exists a traveling wave for any speed $c > c_b$, where c_b is defined in (3.3).

Here we derive some further qualitative properties of traveling waves, concerning monotonicity and identification of their limit at $+\infty$.

The following result states that U has the shape of a bump, and V that of a monotone wave.

Theorem 4.1. *Under the inhibiting assumption (4.1), any traveling wave (U, V) satisfies $V' < 0$ in \mathbb{R} and $U' > 0$ in $(-\infty, \xi_0)$, $U' < 0$ in $(\xi_0, +\infty)$, for some $\xi_0 \in \mathbb{R}$. In addition,*

$$U(+\infty) = 0, \quad V(+\infty) = V_\infty,$$

where $V_\infty \in [0, v_b]$ is a root of $\Psi(0, \cdot)$ and moreover $V_\infty \leq v_*$ from (2.4).

Recall that assumptions (2.6) and (4.1) yield $\Psi(0, 0) = 0$. If $\Psi(0, \cdot)$ has many roots (e.g., if $\Psi(0, \cdot) \equiv 0$), an important issue is the identification of the limiting state V_∞ among them. From a modeling perspective, the quantity $v_b - V_\infty$ measures the amount of social tension dissipated by the movement of social unrest. In the context of epidemiology, $v_b - V_\infty$ represents the total number of individuals that has been infected during the epidemic. Theorem 4.1 provides us with the a priori bound $V_\infty \leq v_*$. To derive a more precise estimate on V_∞ , one can integrate the equation on V (and use $V'(\pm\infty) = 0$) to find

$$c(V_\infty - v_b) = \int_{-\infty}^{+\infty} \Psi(U, V).$$

Analogously, from $U(\pm\infty) = U'(\pm\infty) = 0$, integrating the equation on U gives

$$\int_{-\infty}^{+\infty} U[r(V)f(U) - \omega] = 0.$$

However, this formula is not explicit. In some particular cases (including the SI model (1.1) with $d_2 = 0$), one can obtain a rather explicit expression for V_∞ .

Proposition 4.2. *Let (U, V) be a solution (2.10)-(2.11) with $d_2 = 0$, $f \equiv 1$ and $\Psi(U, V) = UG(V)$, that is*

$$\begin{cases} -d_1 U''(\xi) + cU'(\xi) = U(r(V) - \omega), \\ cV'(\xi) = UG(V), \end{cases}$$

and assume that $G < 0$ on $(0, 1)$. Then, letting Q be a primitive of $v \mapsto \frac{\omega - r(v)}{G(v)}$, there holds that

$$Q(V_\infty) = Q(v_b).$$

In particular, V_∞ does not depend on c , nor on d_1 .

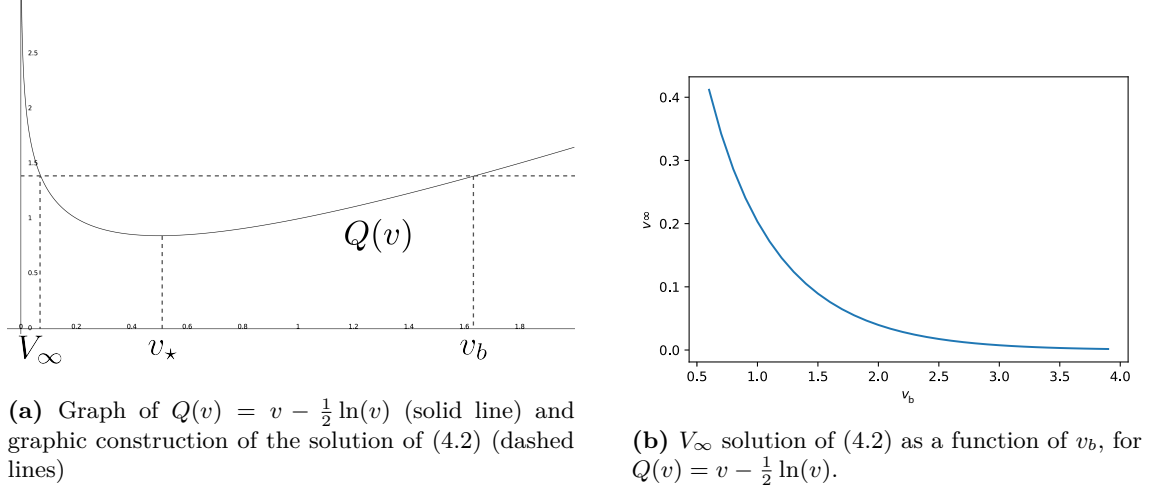


Figure 2

In the particular case of the SI model (1.1) with $d_2 = 0$, we have

$$Q(v) = \frac{1}{\beta}(v - \omega \ln(v)).$$

See Figure 2a. In this case, V_∞ is uniquely determined by the conditions

$$\begin{cases} Q(V_\infty) = Q(v_b), \\ V_\infty \leq v_\star. \end{cases} \quad (4.2)$$

The numerical values of V_∞ as a function of v_b are plotted in Figure 2b for $\beta = \frac{1}{2}$. We see that V_∞ is a decreasing convex function of $v_b \in (v_\star, +\infty)$. From a modeling perspective, it means that the higher the initial level of social tension, the lower the final level of social tension after the burst of a riot.

4.2 Large time behavior for the Cauchy problem

We now turn to the more intricate question of studying the large time behavior of solutions to (2.3). Compared with the previous section on traveling waves, we are only able to establish partial results. We have seen in Section 3.1 that when $v_0 \equiv v_b < v_\star$, perturbations of the steady state $(0, v_b)$ (not necessarily small) eventually disappear as $t \rightarrow +\infty$. On the contrary, if $v_0 \equiv v_b > v_\star$, perturbations do not tend to 0 as $t \rightarrow +\infty$, at least in one of the (u, v) components, see Section 3.2. However, solutions can exhibit many qualitatively diverse behaviors in general. We are able to obtain some informations in the inhibiting case.

Theorem 4.3. *Assume that the inhibiting hypothesis (4.1) holds, that $d_2 > 0$, and that the dimension is $n = 1$ or 2 . Then any solution of (2.3) satisfies*

$$\liminf_{t \rightarrow +\infty} u(t, x) = 0 \quad \text{locally uniformly in } x \in \mathbb{R}^n. \quad (4.3)$$

If in addition $v(t, x)$ converges pointwise to some $v_\infty(x)$ as $t \rightarrow +\infty$, then v_∞ is a constant in $[0, v_\star]$ and $u(t, x) \rightarrow 0$ as $t \rightarrow +\infty$ locally uniformly in $x \in \mathbb{R}^n$.

The first part of the theorem states that the movement of social unrest vanishes along some sequences of time. Moreover, if we assume that v converges as $t \rightarrow +\infty$, then the second part of the theorem states that u converges to 0. This means that only the v component matters in the estimate (3.2) for the case $v_b > v_\star$.

An interesting question is to estimate the final state v_∞ . The following result concerns the homogeneous case, i.e., when $u_0(\cdot)$ is constant

Proposition 4.4. Assume that (4.1) holds. Let (u, v) and (\tilde{u}, \tilde{v}) be the solutions of (2.3) with initial conditions (u_0, v_0) and (u_0, \tilde{v}_0) respectively, where u_0 is constant and $v_0 \equiv v_b$, $\tilde{v}_0 \equiv \tilde{v}_b$. If $v_b > \tilde{v}_b > v_*$, the corresponding final states v_∞ and \tilde{v}_∞ satisfy

$$v_\infty \leq \tilde{v}_\infty < v_*.$$

Moreover,

$$\max_{t>0} u(t) > \max_{t>0} \tilde{u}(t).$$

The above proposition states that the final level v_∞ is decreasing with respect to v_b . From the modeling point of view, it implies that a higher initial level of social tension will lead to a lower final level of social tension. On the contrary, the higher the initial level of social tension, the higher the maximal level of social unrest. This enlightens very well the non monotone structure of the inhibiting case.

4.3 Numerical simulations

Let us illustrate the dynamics of (2.3) in the inhibiting case (4.1) with numerical simulations.

4.3.1 Threshold between calm and riot

Consider the following particular instance of (2.3):

$$\begin{cases} \partial_t u - \partial_{xx} u = u \left[5v(1-u) - \frac{1}{2} \right], \\ \partial_t v - \partial_{xx} v = -uv. \end{cases} \quad (4.4)$$

As for the initial datum, we take $u_0(x) = 0.2(1 - \frac{x^2}{100})_+$, where $(\cdot)_+$ denotes the positive part, and $v_0 \equiv v_b$. Observe that any $v_b \in (0, 1)$ is allowed by the stability hypothesis (2.5). System (4.4) satisfies the inhibiting assumption (4.1). The quantities defined in (2.4) and (2.8) are given by $v_* = \frac{1}{10}$ and $K_b = 5v_b - \frac{1}{2}$.

First, if $v_b < v_*$ we observe in Figure 3 that a triggering event is promptly followed by a return to calm, i.e., u rapidly vanishes. Next, v converges in long time to its initial value v_b . This is in agreement with the property (3.1).

On the contrary, when $v_b = 0.15 > v_*$, Figure 4 shows that the solution does not vanish uniformly in space, but rather develops two traveling waves—one leftward and the other rightward—i.e., two fixed profiles propagating at constant speed. This is in agreement with the discussion in Sections 3.2, 3.3. The profile of u has the shape of a bump, while the profile of v is a decreasing wave, as stated in Theorem 4.1. The fact that the level of SU decays as $t \rightarrow +\infty$, which was expected from Theorem 4.3, means that social movements get extinct after some times. Thus, the dynamics describe a limited-duration movement of social unrest, that we call a *riot*.

4.3.2 Speed of propagation

Let us investigate in more details the dependence of the speed of propagation with respect to v_b on the system

$$\begin{cases} \partial_t u - \partial_{xx} u = u \left[v(1-u) - \frac{1}{3} \right], \\ \partial_t v - \partial_{xx} v = -uv. \end{cases} \quad (4.5)$$

We consider $u_0(x) = 0.2(1 - x^2)_+$ as an initial datum for u , then we will study the asymptotic speed of propagation as the initial datum for v , $v_0 \equiv v_b$, varies in $(0, 1)$.

Let us briefly explain how we numerically compute the speed of propagation. For each simulation and two given times $t_1 = 99$ and $t_2 = 399$, we track the leftmost locations x_i where the solution $u(t_i, \cdot)$ reaches half its supremum, i.e., the value $\frac{1}{2} \sup_{x \in \mathbb{R}} u(t_i, x)$. See Figure 5. Then, we compute the speed as

$$c = \frac{x_2 - x_1}{t_2 - t_1}.$$

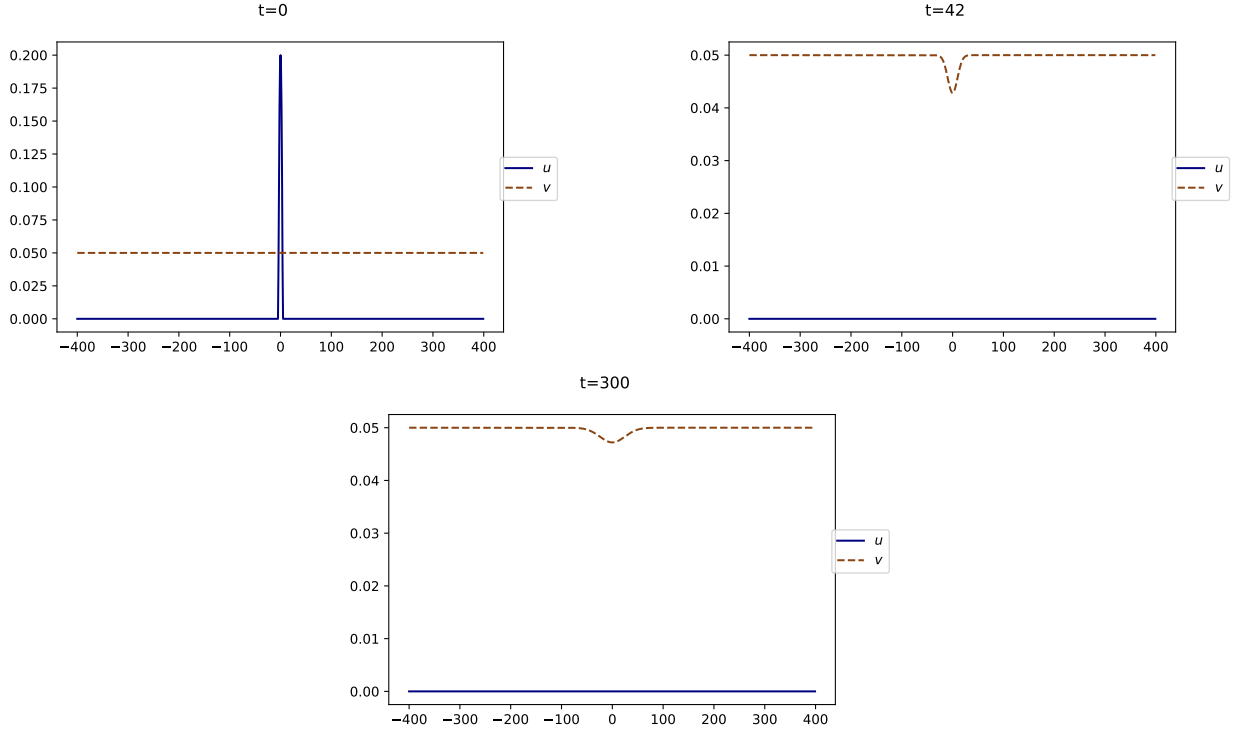


Figure 3: Inhibiting case – return to calm. Snapshots at different times of the solution of (4.4) with $v_b = 0.05 < v_*$. Horizontal axis: space. Blue solid line: $u(t, \cdot)$. Brown dashed line: $v(t, \cdot)$.
[Video: Inhibiting_v0=005.mp4](#)

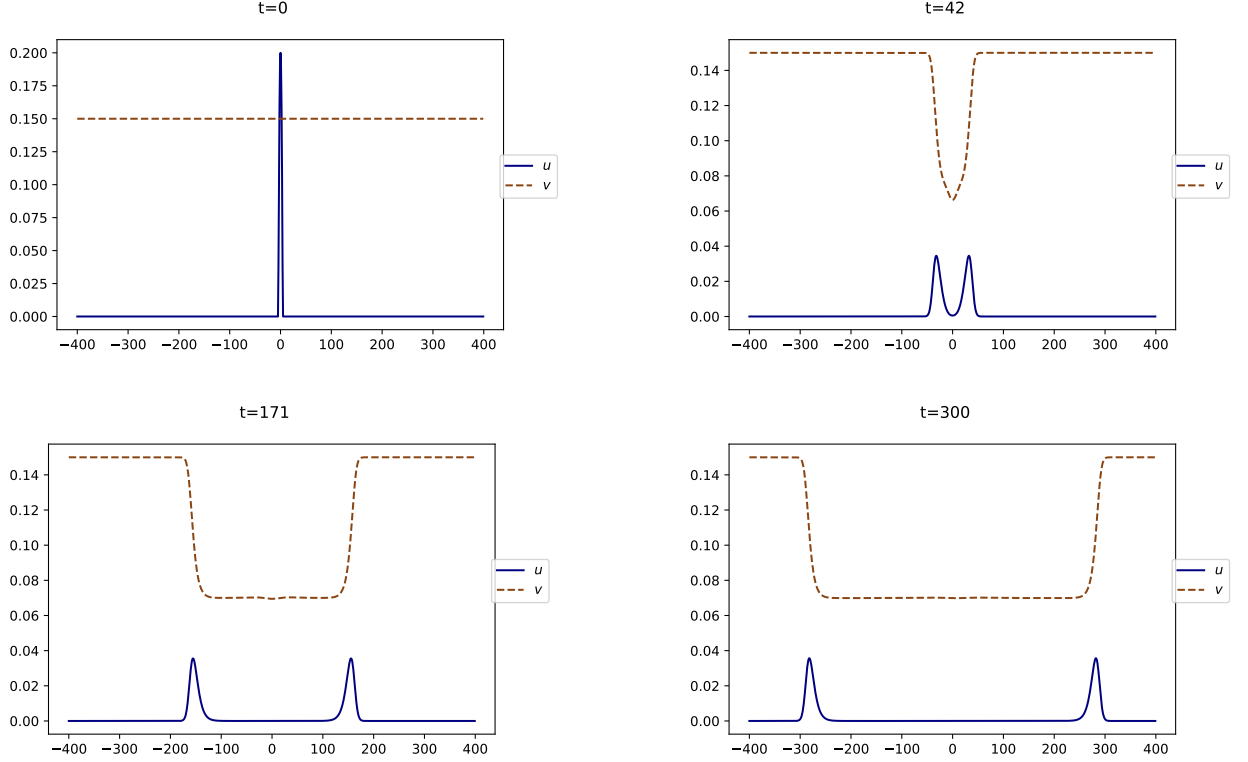


Figure 4: Inhibiting case – riot. Snapshots at different times of the solution of (4.4) with $v_b = 0.15 > v_*$. Horizontal axis: space. Blue solid line: $u(t, \cdot)$. Brown dashed line: $v(t, \cdot)$.
[Video: Inhibiting_v0=015.mp4](#)

We recall that, according to Section 3.3, the speed of propagation of the solution is equal to

$$c_b := 2\sqrt{v_b - \frac{1}{3}}.$$

We plot in Figure 6 the computed speed c and the theoretical speed c_b , and we see that the two speeds are indeed equal.

4.3.3 Eventual level of social tension

As we can see in Figure 4 and Figure 7, the solution (u, v) converges to some $(0, v_\infty)$ as $t \rightarrow +\infty$. We can verify numerically that $v_\infty \leq v_*$, which is in agreement with Theorem 4.3.

It is an interesting question to estimate more precisely the final level of social tension v_∞ . Theoretical results in this direction are given by Propositions 4.2 and 4.4. Let us now study this question with numerical simulations.

We plot in figure Figure 7 the simulation of equation (4.4) with a high initial level of social tension $v_b = 0.9$. Compared with the simulation for $v_b = 0.15$, in Figure 4, we observe that u reaches higher values, that its shape is sharper, and that the speed of propagation is larger.

We also observe in Figure 7 that the eventual level of social tension $v(t = +\infty)$ is very low. To see this more precisely, we plot in Figure 8a the value of v_∞ as a function of v_b on the system (4.4). We observe that v_∞ is indeed a decreasing function of v_b . From a modeling perspective, it means that the higher the initial level of social tension, the lower the final level of social tension. This phenomenon is in agreement with what was observed in Figure 2b for the *SI* model.

Now, let us focus on the dependence of v_∞ with respect to the diffusion on social tension d_2 . We consider (4.5) with a varying diffusion on the second equation, that is,

$$\begin{cases} \partial_t u - \partial_{xx} u = u \left[v(1 - u) - \frac{1}{3} \right], \\ \partial_t v - d_2 \partial_{xx} v = -uv. \end{cases} \quad (4.6)$$

We fix $v_0 \equiv v_b = 0.5$ and $u_0(x) = 0.2(1 - \frac{x^2}{10})_+$. We plot in Figure 8b the value of v_∞ as a function of d_2 . We observe that v_∞ is increasing. From a modeling point of view, it means that the higher the diffusion on the social tension, the higher the final level of social tension. Heuristically, this is explained by the fact that $\lim_{|x| \rightarrow +\infty} v(t, x) = v_b > v_\infty$ and that, the larger d_2 , the more $v(t, x)$ is influenced by its value at far distances.

5 Tension Enhancing - dynamics of a lasting upheaval

The *tension enhancing* structure relies on the following saturation assumptions on f and positivity on Ψ :

$$\begin{cases} f \text{ is strictly decreasing and } f(M) \leq 0 & \text{for some } M > 0, \\ \Psi(u, v) > 0 & \forall u \in (0, M), v \in (0, 1). \end{cases} \quad (5.1)$$

The assumption on f accounts for the saturation effect on the level of social unrest. A typical example is to take $f(u) = M - u$. As a direct consequence, the parabolic comparison principle yields

$$\limsup_{t \rightarrow +\infty} u(t, x) \leq M, \quad \forall x \in \mathbb{R}^n.$$

The assumption on Ψ essentially means that u has a positive feedback on v (we do not assume, however, that $u \mapsto f(u, v)$ is increasing). Again, as a direct consequence of the positivity of Ψ we have that

$$v(t, x) > v_0 \equiv v_b \quad \forall t > 0, x \in \mathbb{R}^n.$$

A typical example of the *tension enhancing* case is the cooperative system

$$\begin{cases} \partial_t u - d_1 \Delta u = u[v(1 - u) - \omega], \\ \partial_t v - d_2 \Delta v = uv(1 - v), \end{cases}$$

obtained by taking $r(u, v) = v$, $f(u, v) \equiv 1 - u$, $\Psi(u, v) = uv(1 - v)$ in (2.3).

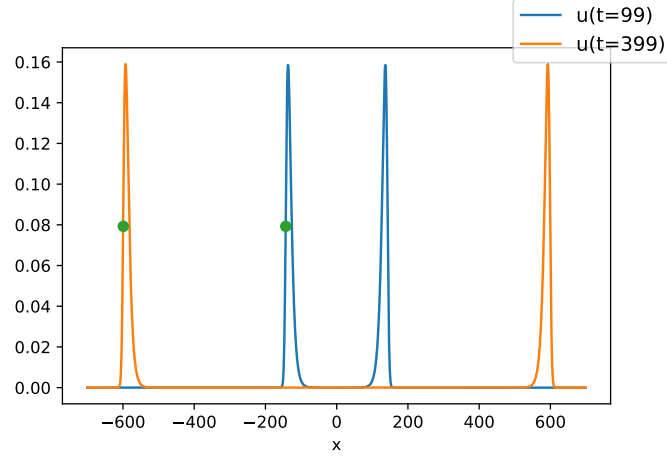


Figure 5: Illustration of the method to compute the speed numerically. The horizontal coordinates of the green circles represent respectively the leftmost locations x_1 and x_2 where $u(t_1, \cdot)$ and $u(t_2, \cdot)$ reach half their supremum. The simulation is performed on (4.5) with $v_b = 0.9$.

[Video: Speed_v0=09.mp4](#)

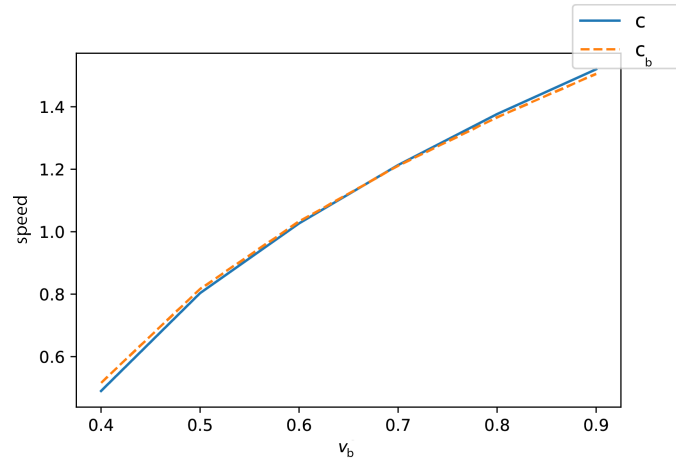


Figure 6: Inhibiting case – speed of propagation as a function of v_b . Blue solid line: empirical speed c computed numerically via the solution of (4.5). Dashed orange line: theoretical speed $c_b = 2\sqrt{v_b - \frac{1}{3}}$.

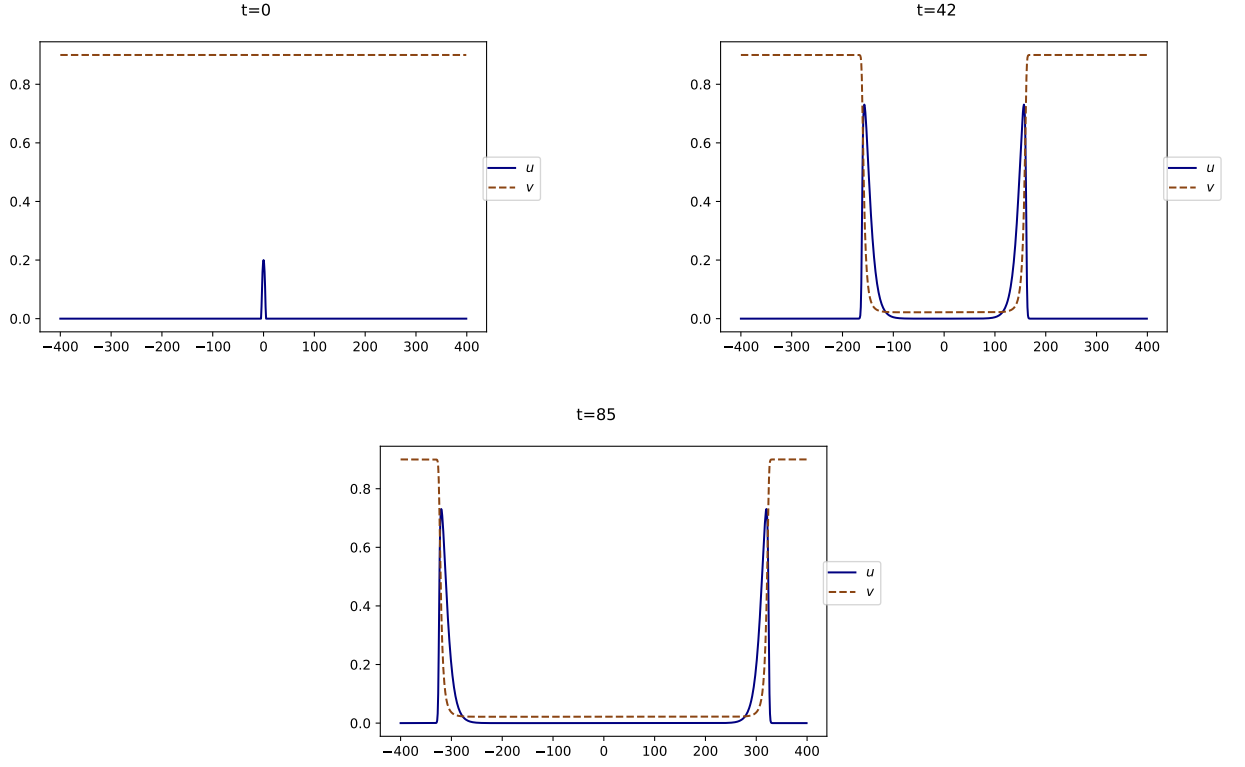


Figure 7: Inhibiting case – strong riot. Snapshot at different times of the solution of (4.4) with $v_b = 0.9 > v_*$ (compare with Figure 4 where $v_b = 0.15$). Horizontal axis: space. Blue solid line: $u(t, \cdot)$. Brown dashed line: $v(t, \cdot)$. [Video: Inhibiting_v0=09.mp4](#)

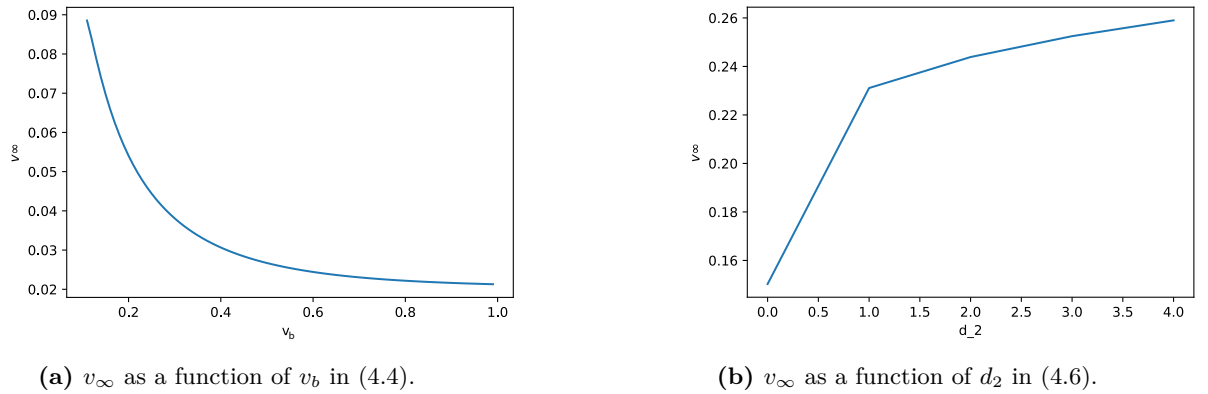


Figure 8: Inhibiting case – eventual level of social tension $v_\infty = \lim_{t \rightarrow +\infty} v(t, \cdot)$ as a function of the parameters for the solution of (4.6).

The *tension enhancing* assumption typically grasps the dynamics of a persisting movement of social unrest, that we refer to here as a *lasting upheaval*. A good heuristic of the behavior of the model is given by a formal analysis of the underlying *ODE* system. Taking u_0 constant implies that the solutions u and v of (2.3) do not depend on x . If the initial level of social tension is above the threshold $v_* = \omega$ from (2.4), then any *triggering event* ignites a *burst* of social unrest. The level of social tension then *increases*, which enhances the growth of social unrest. Eventually, both the level of social tension and social unrest converge to an excited state, $v \rightarrow 1$ and $u \rightarrow u_*(1) = 1 - \omega$ from definition (2.9).

We begin by stating qualitative properties for the traveling waves, then we investigate the large time behavior of solutions to (2.3). On this latter question, we obtain more complete results than in the inhibiting case (Section 4), since we prove that the solution converges to an excited state as $t \rightarrow +\infty$. The results are illustrated by numerical simulations.

5.1 Traveling waves

Let us first discuss the existence and non-existence of traveling solutions of (2.10)-(2.11) using the results of [17]. Consider the function $\gamma : [c_1, +\infty) \rightarrow \mathbb{R}$ defined by

$$\gamma(c) := \frac{\sqrt{c^2 - c_b^2} - \sqrt{c^2 - c_1^2}}{2c},$$

where c_b and c_1 are defined in (3.3). Because $c_b < c_1$, we have that γ is positive and decreasing, with $\gamma(c_1) = \frac{1}{2}\sqrt{1 - \frac{c_b^2}{c_1^2}}$ and $\gamma(+\infty) = 0$. Let us define

$$\bar{c} := \inf \{c \geq c_1 : d_2\gamma(c) \leq d_1\} \in [c_1, +\infty).$$

We point out that

$$\bar{c} = \begin{cases} c_1, & \text{if } d_2\gamma(c_1) \leq d_1, \\ \gamma^{-1}\left(\frac{d_1}{d_2}\right), & \text{otherwise.} \end{cases}$$

Recalling that the sign of $v_b - v_*$ (from definition (2.4)) coincides with the one of K_b (from (2.8)), [17, Theorem 4] imply that, under the assumptions (5.1) and $v_b > v_*$, the following hold:

- there exists no traveling wave with speed $c < c_b$;
- there exists a traveling wave with any speed $c > \bar{c}$.

In particular, if d_2 is sufficiently small, then $\bar{c} = c_1$, and so there exists a traveling wave for any speed greater than c_1 .

The following result deals with the shape of the traveling waves.

Theorem 5.1. *Under the enhancing assumption (5.1), any traveling wave satisfies $U' > 0$, $V' > 0$ in \mathbb{R} and*

$$U(+\infty) = u_*(1) := f^{-1}\left(\frac{\omega}{r(1)}\right), \quad V(+\infty) = 1.$$

5.2 Large time behavior for the Cauchy problem

In the previous section, we have identified the limits of traveling waves as $\xi \rightarrow +\infty$. We now show that the same limits hold for the solution of (2.3) as $t \rightarrow +\infty$.

Theorem 5.2. *Assume that (5.1) holds and that $v_b > v_*$. Then any solution of (2.3) with $v_0 \equiv v_b$ and u_0 compactly supported satisfies*

$$\lim_{t \rightarrow +\infty} u(t, x) = u_*(1) := f^{-1}\left(\frac{\omega}{r(1)}\right), \quad \lim_{t \rightarrow +\infty} v(t, x) = 1,$$

locally uniformly in $x \in \mathbb{R}^n$.

This theorem states that the level of social unrest converges to a sustainable excited state $u_*(1)$. From a modeling point of view, this corresponds to a persisting social movement, that we refer to as a *lasting upheaval*.

5.3 Numerical simulations

In this section we provide some numerical illustrations of the dynamics of system (2.3) in the enhancing case (5.1).

5.3.1 Threshold between calm and lasting upheaval

Let us consider the following particular instance of (2.3) satisfying the enhancing assumption (5.1):

$$\begin{cases} \partial_t u - \partial_{xx} u = u \left[v(1 - u) - \frac{1}{3} \right], \\ \partial_t v - \partial_{xx} v = uv(1 - v), \end{cases} \quad (5.2)$$

with initial condition $u_0(x) = 0.2(1 - x^2)_+$ and $v_0 \equiv v_b$ ranging in $(0, 1)$. In this case we have $v_\star = 1/3$ and $K_b := v_b - 1/3$.

Figure 9 refers to the case $v_b < v_\star$. We observe there that a triggering event is promptly followed by a return to calm, namely, u rapidly vanishes. Next, v converges in long time to its initial value v_b . This is in agreement with the discussion in Section 3.1. Let us emphasize, however, that this is only true when considering a sufficiently small initial condition $u_0(x)$, see Section 5.3.2 for more details.

On the contrary, if $v_b > v_\star$, a small triggering event ignites a burst of social unrest that spreads through space, as can be seen on Figure 10. This is in agreement with Sections 3.2 and 3.3. More precisely, the simulation shows that the solution converges to two traveling waves, one leftwards and the other one rightwards, i.e., two fixed profiles moving at a constant speed. The profiles for both u and v have the shape of monotone waves, as stated in Theorem 5.1. In addition, the solution converges pointwise to $(u_\star(1), 1)$ as $t \rightarrow +\infty$, in agreement with Theorem 5.2.

Since the asymptotic state as $t \rightarrow +\infty$ features a positive level of activity, the dynamics describe a persisting movement of social unrest, that we call a *lasting upheaval*.

5.3.2 Magnitude of the triggering event

In the *tension enhancing* case, the magnitude of the triggering event (i.e., the size of $u_0(x)$) may be of crucial importance to determine the regime of the dynamics when $v_0 \equiv v_b < v_\star$. This has to be put in contrast with *tension inhibiting* case (described in Section 4) for which the regime of the dynamics do not depends on the size of $u_0(x)$.

Figure 11 depicts two distinct dynamics for system (5.2) corresponding to $v_b = 0.3 < v_\star = 1/3$: the initial condition $u_0(x) = 0.1(1 - x^2)_+$ exhibits a *return to calm*, see Figure 11a, whereas $u_0(x) = 0.5(1 - x^2)_+$ ignites a lasting upheaval, see Figure 11b.

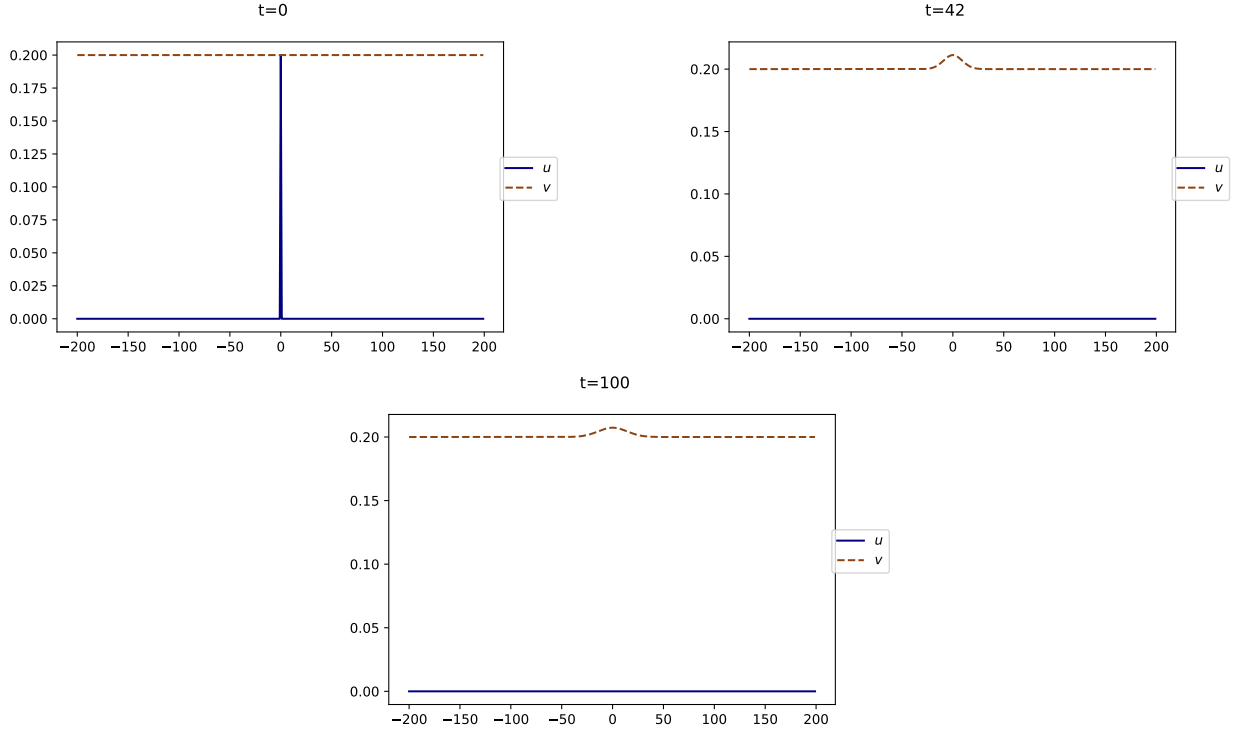


Figure 9: Enhancing case – return to calm. Snapshots at different times of the space distribution of the solution of (5.2) with $v_b = 0.2 < v_*$. Horizontal axis: space. Blue solid line: $u(t, \cdot)$. Brown dashed line: $v(t, \cdot)$. [Video: Enhancing_v0=02.mp4](#)

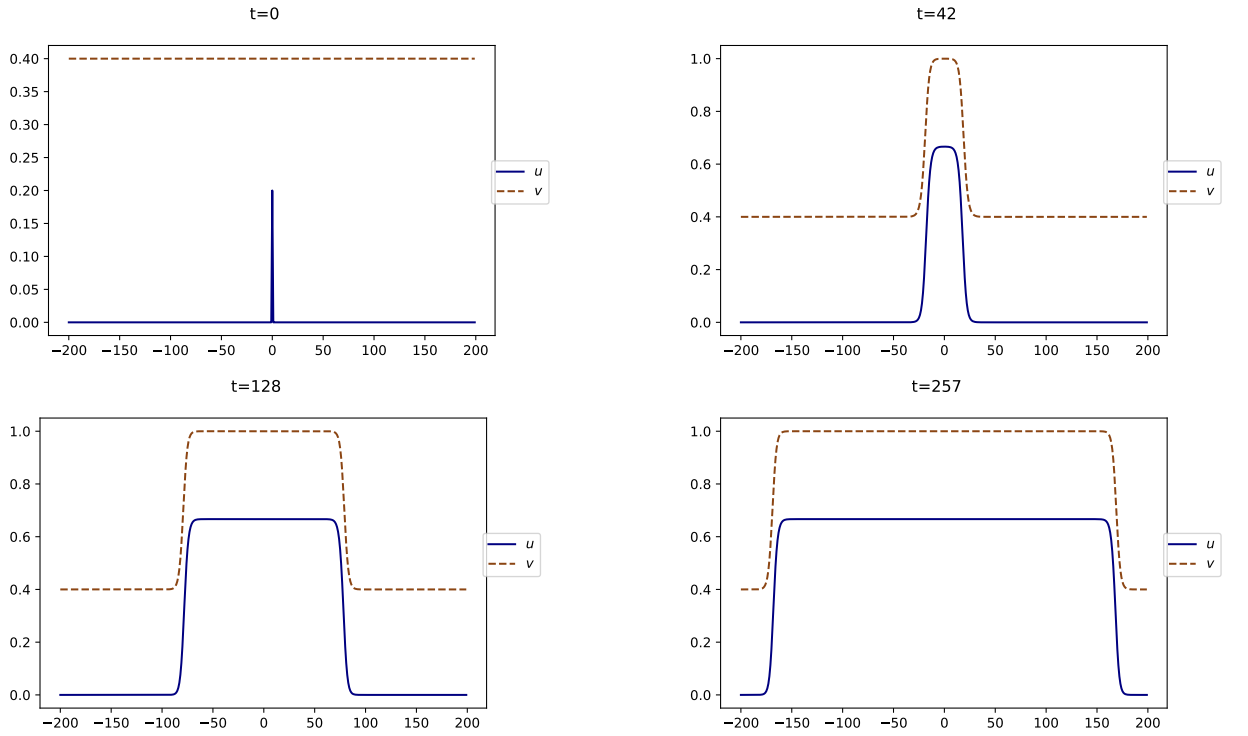
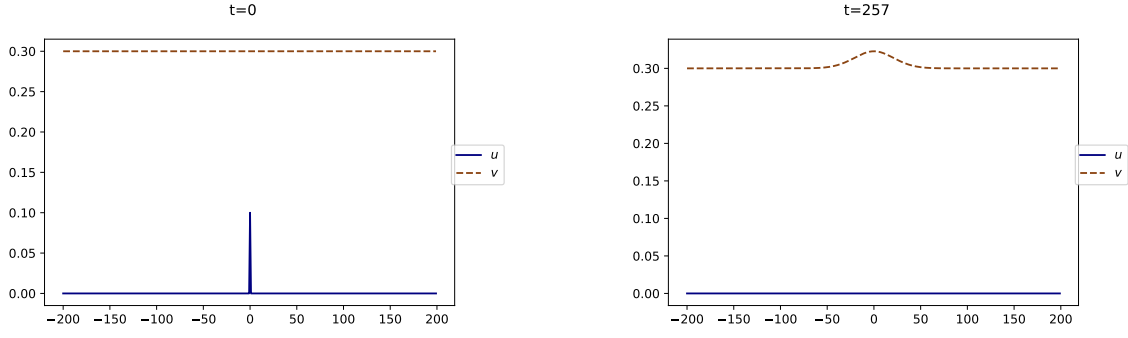
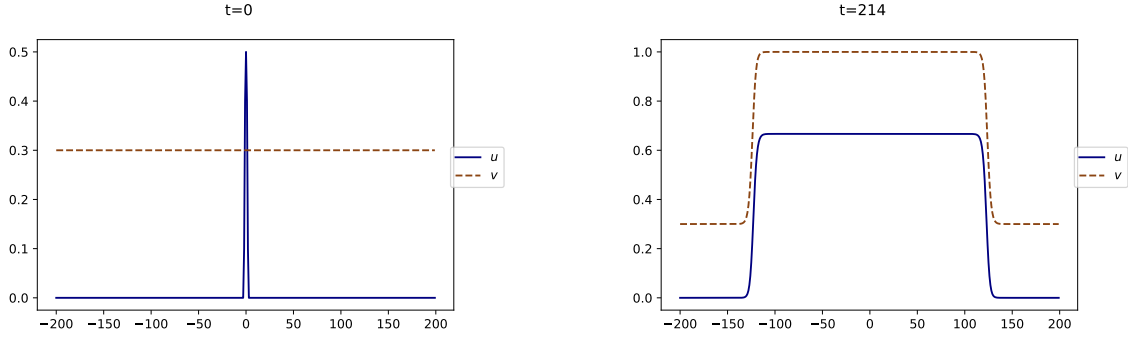


Figure 10: Enhancing case – lasting upheaval. Snapshots at different times of the solution of (5.2) with $v_b = 0.4 > v_*$. Horizontal axis: space. Blue solid line: $u(t, \cdot)$. Brown dashed line: $v(t, \cdot)$. [Video: Enhancing_v0=04.mp4](#)



(a) Calm for $u_0(x) = 0.1(1 - x^2)_+$. [Video: Triggering_u0=01.mp4](#)



(b) lasting upheaval for $u_0(x) = 0.5(1 - x^2)_+$. [Video: Triggering_u0=05.mp4](#)

Figure 11: Enhancing case – influence of the magnitude of the triggering event. Snapshots at different times of the solution of (5.2) with $v_b = 0.3 < v_*$. Horizontal axis: space. Blue solid line: $u(t, \cdot)$. Brown dashed line: $v(t, \cdot)$.

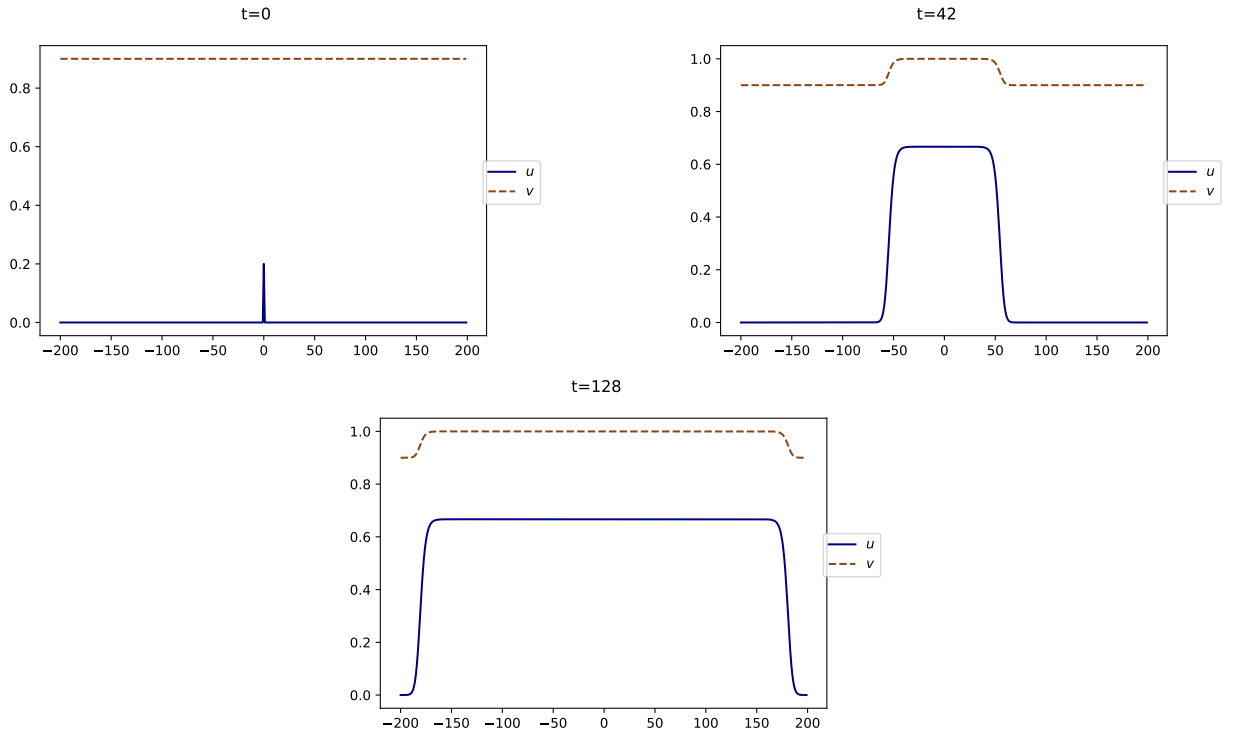


Figure 12: Enhancing case – lasting upheaval. Simulation of (5.2) with $v_b = 0.9 > v_*$. Horizontal axis: space. Blue solid line: $u(t, \cdot)$. Brown dashed line: $v(t, \cdot)$. [Video: Enhancing_v0=09.mp4](#)

The phenomenon depicted by Figure 11 can be explained by the following heuristic: if u_0 is

large enough, then $u(t, \cdot)$ remains at high values for a sufficiently long time so that v increase and reach values above the threshold v_* .

5.3.3 Speed of propagation

We see in Figure 10 that, if the initial level of social tension v_b is above the threshold v_* , the solution of (5.2) propagates through space at a constant speed. If we increase the initial social tension, we observe that the solution propagates faster through space. See Figure 12 for a numerical simulation of (5.2) with $v_b = 0.9$.

To see this phenomenon more clearly, we plot the speed of propagation c of the solution of (5.2) as a function of v_b in Figure 13a (the speed is computed with the method presented in Section 4.3.2). We see that c is indeed an increasing function of v_b .

The theoretical result presented in Section 3.3 states that c ranges in (c_b, c_1) defined in (3.3). This is confirmed numerically in Figure 13a.

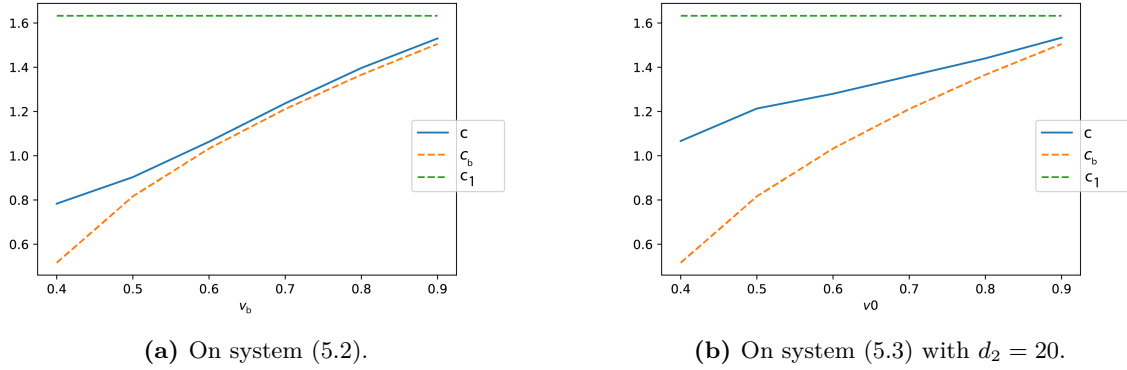


Figure 13: Enhancing case – speed of propagation. Blue solid line: empirical speed c . Dashed lines: theoretical bounds on the speed, $c_b = 2\sqrt{v_b - \frac{1}{3}}$ and $c_1 = 2\sqrt{1 - \frac{1}{3}}$.

Figure 13a could suggest that $c \approx c_b$, or that c does not depend on the equation on v (i.e. d_2 and Ψ) like in the inhibiting case (Section 4.3.2). However, numerical experiment shows that it is not the case in general. This is a substantial difference with the inhibiting case, for which $c = c_b$. To see this, let us consider the same system (5.2) with a diffusion coefficient d_2 on the second equation:

$$\begin{cases} \partial_t u - \partial_{xx} u = u \left[v(1 - u) - \frac{1}{3} \right], \\ \partial_t v - d_2 \partial_{xx} v = uv(1 - v). \end{cases} \quad (5.3)$$

We plot in Figure 13b the speed of propagation c of the solution of (5.3) with $d_2 = 20$ as a function of v_b . We see that c and c_b largely differ, especially for small values of v_b . This is a numerical evidence that v_b depends on d_2 . Fixing $v_b = 0.9$, we see on Figure 14a that c is indeed an increasing function of d_2 . Again, this has to be put in contrast with the inhibiting case, for which $c = c_b$ does not depend on d_2 .

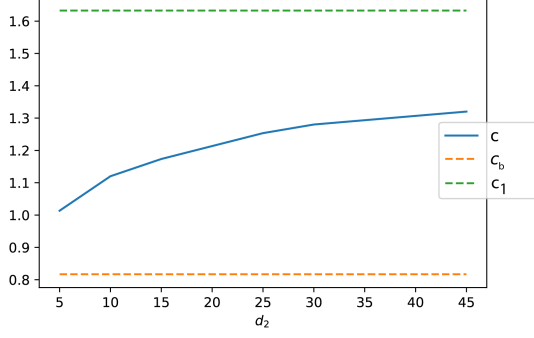
Let us now investigate how the speed depends on the magnitude of Ψ . Consider the analogous of system (5.2) with a variable magnitude for the reaction term in the second equation, namely,

$$\begin{cases} \partial_t u - \partial_{xx} u = u \left[v(1 - u) - \frac{1}{3} \right], \\ \partial_t v - \partial_{xx} v = kuv(1 - v), \end{cases} \quad (5.4)$$

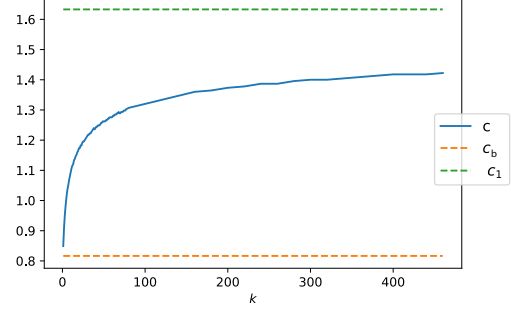
where $k \geq 0$ is a parameter, and $v_b = 0.5$. We plot the speed c as a function of k in Figure 14b. We see that c is an increasing function of k , and so that it indeed depends on the magnitude of Ψ .

These observations motivate the following questions.

Open problem: Do we have $\lim_{d_2 \rightarrow +\infty} c = c_1$ in (5.3)? Do we have $\lim_{k \rightarrow 0} c = c_b$ or $\lim_{k \rightarrow +\infty} c = c_1$ in (5.4)?



(a) Speed c as a function of d_2 on the system (5.3) with $v_b = 0.9$.



(b) Speed c as a function of k on the system (5.4) with $v_b = 0.5$.

Figure 14: Enhancing case – dependence of the speed c on the parameters d_2 and Ψ

6 Mixed cases

We propose in this section to focus on some particular instances of (2.3) which exhibit more complex behaviors. We begin with a model featuring a double threshold phenomenon which can give rise to both ephemeral riots and lasting upheaval. Next, we present other models where oscillating traveling waves appear.

6.1 Double threshold: calm-riot-lasting upheaval

Consider the system

$$\begin{cases} \partial_t u - \partial_{xx} u = u \left[v(1-u) - \frac{1}{3} \right], \\ \partial_t v - d_2 \partial_{xx} v = uv(1-v)(v - \frac{1}{2}), \end{cases} \quad (6.1)$$

and some initial conditions $u_0(x) \geq 0$ and $v_b \in (0, 1)$. We find $v_* = 1/3$ from definition (2.4). Depending on the value of v_b , we have the following dichotomy:

- if $v_0 \equiv v_b < 1/2$: the system is tension inhibiting (4.1),
- if $v_0 \equiv v_b > 1/2$: the system is tension enhancing (5.1).

Indeed, note that $v_0 < 1/2$ implies that $v(t, x) \in (0, 1/2)$ and $v_0 > 1/2$ that $v(t, x)$; one can thus restrict Ψ to a suitable range where $\Psi(\cdot, v(t, x))$ is either positive or negative.

We can then apply the results of the previous sections to infer that a small *triggering event* can lead to three different situations:

- For a small initial level of social tension $v_b \in (0, v_*)$: *return to calm* (Section 3).
- For an intermediate initial level of social tension $v \in (v_*, 1/2)$: *burst of an ephemeral riot* (Section 4).
- For a high initial level of social tension $v \in (1/2, 1)$: *burst of a lasting upheaval* (Section 3).

From the modeling point of view, this double threshold phenomenon means that, in the model (6.1), the initial level of social tension determines whether a small triggering event ignites a social movement, and also whether the movement will be ephemeral or persisting.

We propose to illustrate this double threshold phenomenon with numerical simulations of (6.1). We take $v_0 \equiv v_b \in (0, 1)$ and $u_0(x) = 0.1(1 - x^2)_+$. Figure 15 illustrates the *return to calm* for $v_b = 0.3$; Figure 16 the propagation of a *riot* for $v_b = 0.4$; Figure 17 the propagation of a *lasting upheaval* for $v_b = 0.6$.

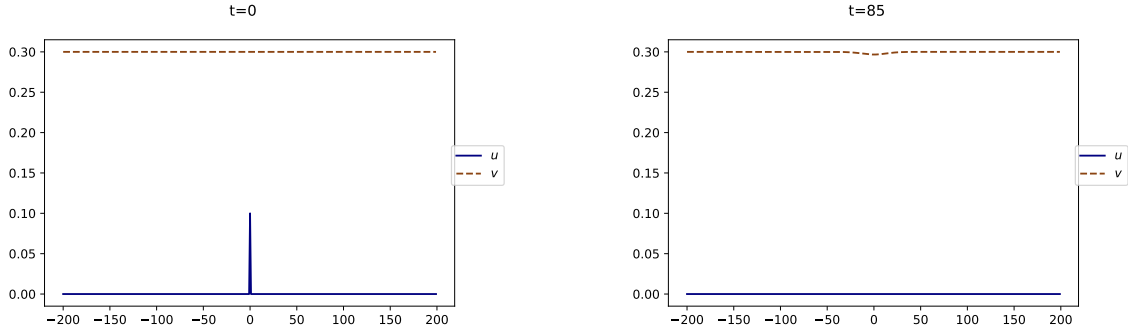


Figure 15: Mixed Case – Calm. Snapshots at different times of the solution of (6.1) with $v_b = 0.3 < v_*$. Horizontal axis: space. Blue solid line: $u(t, \cdot)$. Brown dashed line: $v(t, \cdot)$.
[Video: Mixed_V0=03.mp4](#)

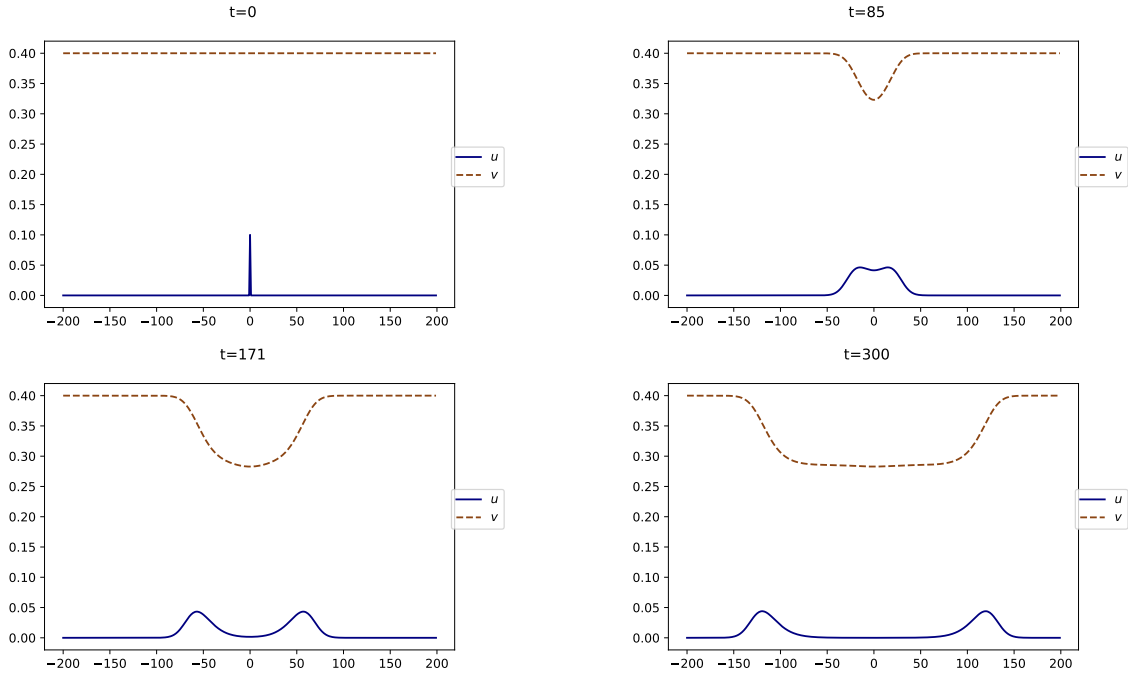


Figure 16: Mixed Case – riot. Snapshots at different times of the solution of (6.1) with $v_b = 0.4 \in (v_*, 1/2)$. Horizontal axis: space. Blue solid line: $u(t, \cdot)$. Brown dashed line: $v(t, \cdot)$.
[Video: Mixed_V0=04.mp4](#)

6.2 Oscillating traveling waves

We saw in Sections 4.1, 5.1 that the traveling wave can have the shape of a bump or a monotonic wave. Yet, some traveling waves may have a more complex shape. For example, consider the following particular instance of (2.3)

$$\begin{cases} \partial_t u - \partial_{xx} u = u \left[v(1-u) - \frac{1}{3} \right], \\ \partial_t v - \partial_{xx} v = uv(1-v)(v-10u). \end{cases} \quad (6.2)$$

We see in Figure 18 that the solution converges to a traveling wave which features damped oscillations on its tail.

We suspect that some well-chosen parameters could generate traveling wave with undamped oscillation; yet, we are not able to produce such an example.

6.3 Magnitude of the triggering event and terraces

As described in Section 5.3.2, when the system is not *tension inhibiting*, the magnitude of the triggering event (i.e. the size of u_0) may be of crucial importance to determine the regime of the dynamics when $v_0 \equiv v_b < v_*$.

The same phenomenon may occur even in the case $v_0 \equiv v_b > v_*$. Indeed, consider the system

$$\begin{cases} \partial_t u - \partial_{xx} u = u \left[v(1-u) - \frac{1}{3} \right], \\ \partial_t v - \partial_{xx} v = uv(1-v)(v+u-\frac{1}{2}). \end{cases} \quad (6.3)$$

We find $v_* = 1/3$ from definition (2.4). Fixing $v_0 \equiv v_b > v_*$ close to the threshold $1/2$, we expect that the magnitude of the triggering event determines whether the dynamics give rise to an ephemeral riot or a lasting upheaval. We see in Figure 19a that, taking $v_b = 0.4$ and $u_0(x) = 0.1(1 - \frac{x^2}{10})_+$, system (6.3) gives rise to an ephemeral *riot*. On the contrary, with the same initial level of social tension $v_b = 0.4$, but with a larger triggering event $u_0(x) = 0.5(1 - \frac{x^2}{10})_+$, we observe a *lasting upheaval* in Figure 19b.

There are also some examples where a sufficiently large triggering event generates a fast riot followed by a slower persisting upheaval. Mathematically speaking, this consists of a terrace, that is, the superposition of two traveling waves traveling at different speeds. Consider

$$\begin{cases} \partial_t u - \partial_{xx} u = u \left[v(1-u) - \frac{1}{3} \right], \\ \partial_t v - \partial_{xx} v = \frac{1}{2} uv(1-v)(v+u-\frac{2}{3}). \end{cases} \quad (6.4)$$

with $v_b = 0.44$ and $u_0 = \varepsilon(1 - x^2)_+$. Taking $\varepsilon = 1.5$, we see in Figure 20 that the dynamics correspond to that of a riot. However, if we consider a triggering event with a larger magnitude by taking $\varepsilon = 1.6$, we observe a terrace in Figure 21, featuring an ephemeral riot followed by a lasting upheaval (the traveling speed of the upheaval equals approximately half the one of the riot).

The same phenomenon can also be observed on the following example

$$\begin{cases} \partial_t u - \partial_{xx} u = u \left[v(1-u) - \frac{1}{3} \right], \\ \partial_t v - \partial_{xx} v = u \left(u - \frac{1}{4} \right) v(1-v). \end{cases}$$

for $v_b = 0.5$ and $u_0 = \varepsilon(1 - x^2)_+$. Loosely speaking, this system can be interpreted as *tension inhibiting* for $u < 1/4$ and *tension enhancing* for $u > 1/4$. We observe a riot for $\varepsilon = 0.5$ ([video: Terrace2_eps=05.mp4](#)) and a terrace consisting of a riot followed by a lasting upheaval for $\varepsilon = 0.6$ ([video: Terrace2_eps=06.mp4](#)).

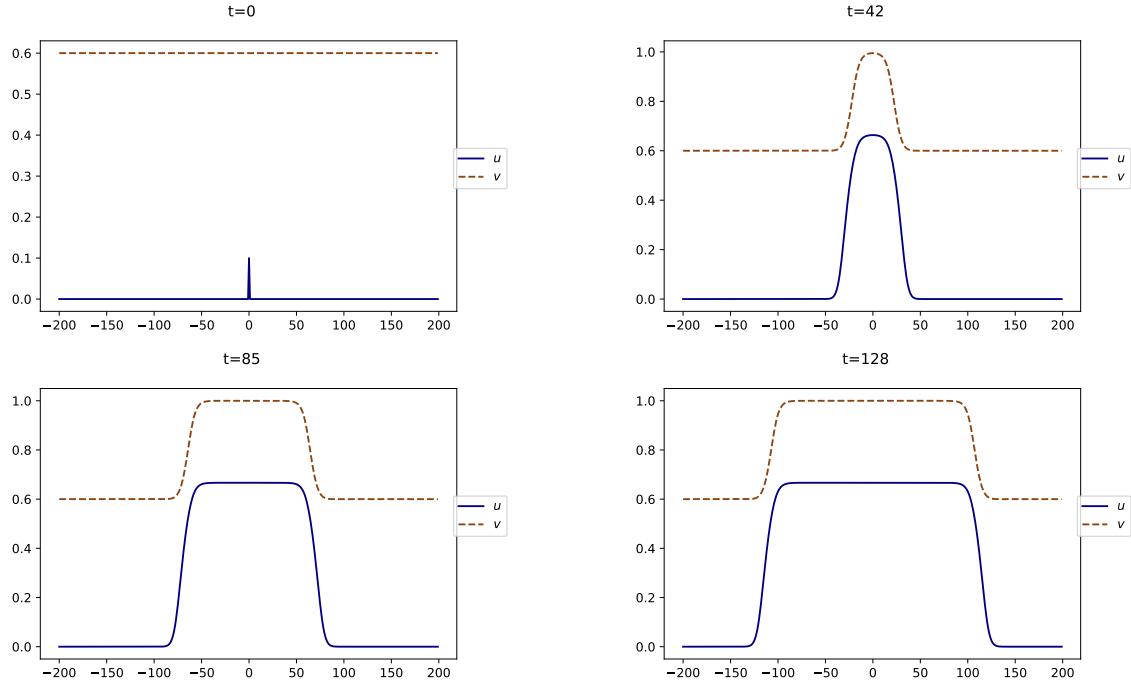


Figure 17: Mixed Case – lasting upheaval. Snapshots at different times of the solution of (6.1) for $v_b = 0.6 \in (1/2, 1)$. [Video: Mixed_V0=06.mp4](#)

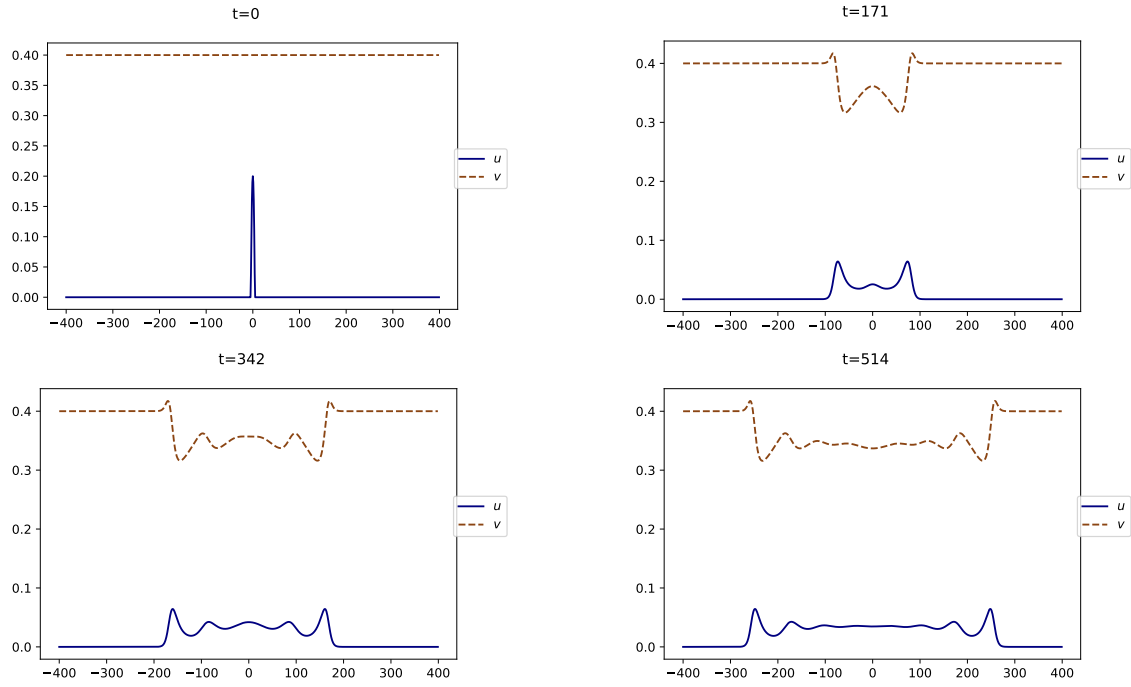
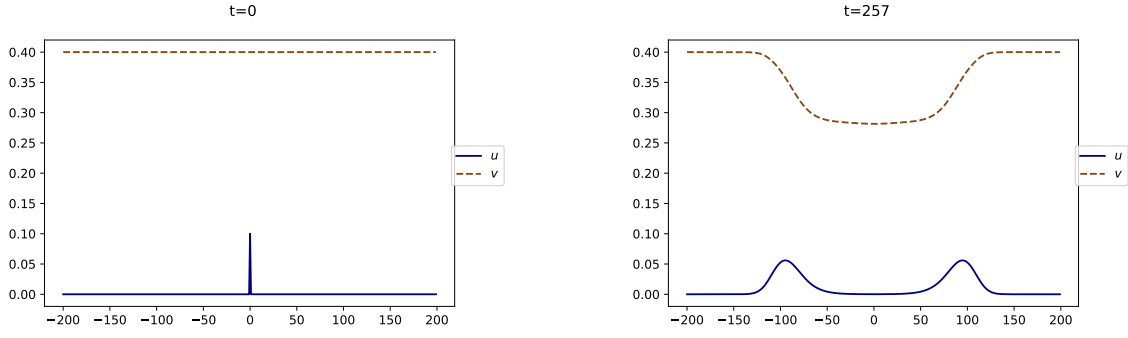
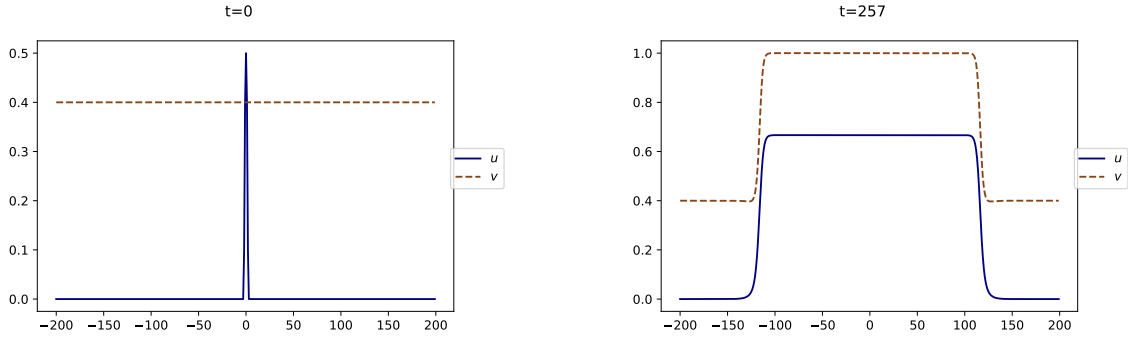


Figure 18: Mixed Case – Oscillating traveling wave. Snapshots at different times of the solution of (6.2) for $v_b = 0.4$ and $u_0(x) = 0.2(1 - \frac{x^2}{100})_+$. [Video: Oscillation_v0=04.mp4](#)



(a) Riot for $u_0(x) = 0.1(1 - \frac{x^2}{10})_+$. [Video: Threshold_Riot-Revolution_u0=01.mp4](#)



(b) lasting upheaval for $u_0(x) = 0.5(1 - \frac{x^2}{10})_+$. [Video: Threshold_Riot-Revolution_u0=05.mp4](#)

Figure 19: Mixed case – influence of the magnitude of the triggering event. Snapshots at different times of the solution of (6.3) with $v_b = 0.4$

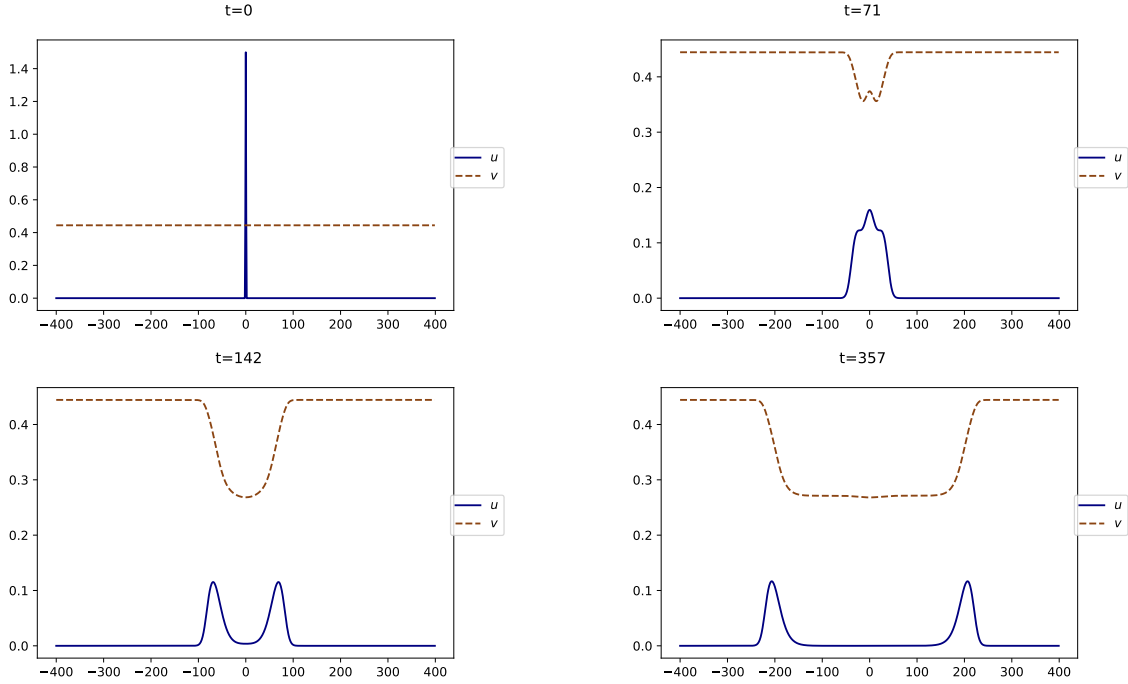


Figure 20: No terrace: simple riot. Snapshots at different times of the solution of (6.4) for $v_b = 0.44$ and $u_0(x) = 1.5(1 - x^2)_+$. [Video: Terrace_eps=15e-1.mp4](#)

7 Spatially heterogeneous models

Data show that the dynamics of social unrest is highly influenced by many factors that are not homogeneous in space, such as the density of population, poverty, etc. See, e.g. [22]. An interesting extension of our model is to introduce spatial heterogeneity in the system (2.3). In this section, we propose some possible ways to do this and provide some numerics.

7.1 Gap problem

The first approach to account for space heterogeneity is to assume that the function $\Phi(u, v)$ (which, we recall, stands for the growth of the level of social unrest u) depends explicitly on the space variable x . We may assume that some areas in space are not favorable to the growth of social unrest. It is then an interesting problem to determine whether a propagating movement of social unrest can overcome those areas.

For some interval $\mathcal{K} := (a, a + L)$, representing the *gap* (or the *obstacle*), we choose Φ of the form

$$\Phi(x, u, v) = u [r(v)f(u)\mathbb{1}_{x \notin (a, a+L)} - \omega].$$

Namely, in dimension $n = 1$, we consider the system

$$\begin{cases} \partial_t u - d_1 \partial_{xx} u = u [r(v)f(u)\mathbb{1}_{x \notin (a, a+L)} - \omega], \\ \partial_t v - d_2 \partial_{xx} v = \Psi(u, v). \end{cases}$$

We ask the following question: is there a threshold on the length L of the obstacle above which the propagation of the solution is blocked?

First, let us remark that, if $v_0 \equiv v_b > v_*$, then our system enjoys a *Hair-Trigger* effect: it means that arbitrarily small initial conditions ignites a social movement (see Sections 3.1 and 3.2). Since, for all $t > 0$, we have that $u(t, \cdot) > 0$, we deduce that there exists no gap that can block the propagation. We illustrate this remark with a numerical simulation on Figure 22 for the system (4.5), that is

$$\begin{cases} \partial_t u - \partial_{xx} u = u \left[v(1 - u)\mathbb{1}_{x \notin (60, 60+L)} - \frac{1}{3} \right], \\ \partial_t v - \partial_{xx} v = -uv, \end{cases} \quad (7.1)$$

with $v_b = 0.6$ (we recall that $v_* = 1/3$) and $u_0(x) = 0.2(1 - x^2)_+$. We see on Figure 22 that a riot begins to propagate, but then fades as it reaches the obstacle. However, after some times, the riot grows again and continue to propagate beyond the obstacle.

However, if we are in a situation where $v_0 \equiv v_b < v_*$ but u_0 is large enough to triggers a social movement (as described in Sections 5.3.2, 6.3), there might exists a length L above which the gap blocks the propagation. Let us consider the following system

$$\begin{cases} \partial_t u - \partial_{xx} u = u \left[v(1 - u)\mathbb{1}_{x \notin (60, 60+L)} - \frac{1}{3} \right], \\ \partial_t v - \partial_{xx} v = 6uv(1 - v)(v + 10u - \frac{2}{3}), \end{cases} \quad (7.2)$$

with $v_b = 0.3$ and $u_0(x) = (1 - \frac{x^2}{10})_+$. We plot in Figure 23 a numerical simulation of the above system for $L = 40$. We observe that an upheaval propagates until it reaches the obstacle. Then, after some time, the upheaval manages to overpass the obstacle and continue to propagate. If now we increase the length of the gap to $L = 60$, we see in Figure 24 that the spreading of the upheaval is blocked by the gap (even after a long time).

Of course, one could also consider that Ψ depends on the space variable x , but we omit this case for conciseness.

7.2 Non-uniform initial social tension

So far, we have only dealt with a constant initial level of social tension $v_0 \equiv v_b$ (although more general results are available in [17] when $v_0 - v_b$ is compactly supported). Another way to encode space heterogeneity in our model is to consider the case of a non-constant initial level of social tension v_0 . This case is relevant from a modeling perspective, since the social tension may indeed

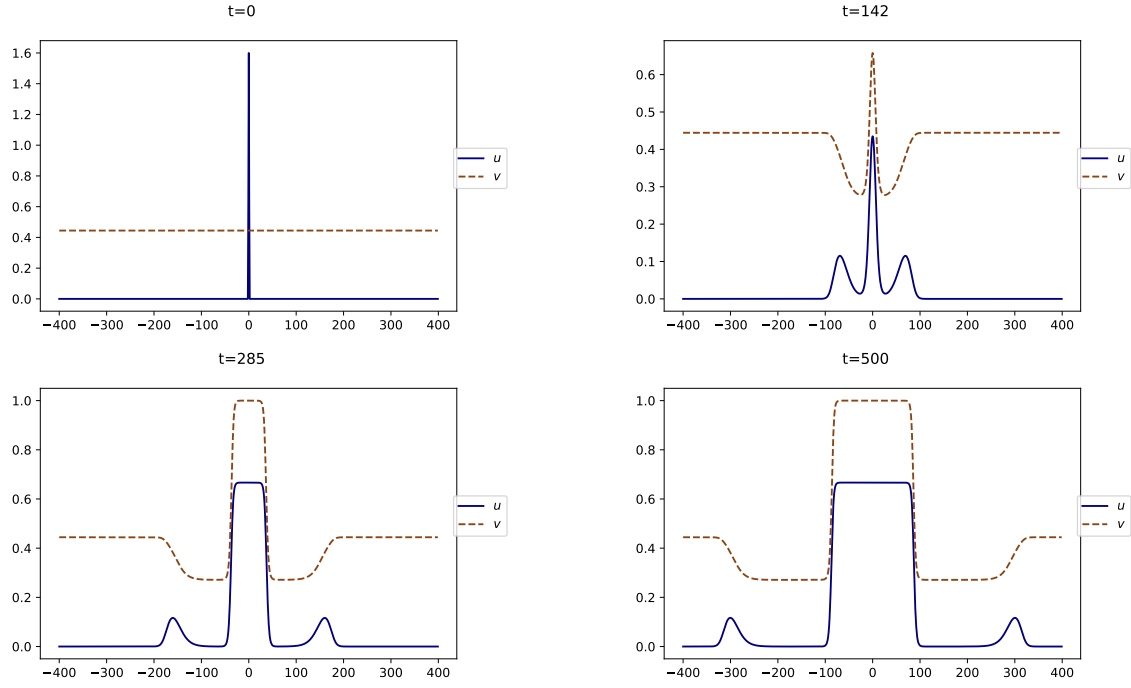


Figure 21: Terrace: riot followed by a lasting upheaval. Snapshots at different times of the solution of (6.4) for $v_b = 0.44$ and $u_0(x) = 1.6(1 - x^2)_+$. [Video: Terrace_eps=16e-1.mp4](#)

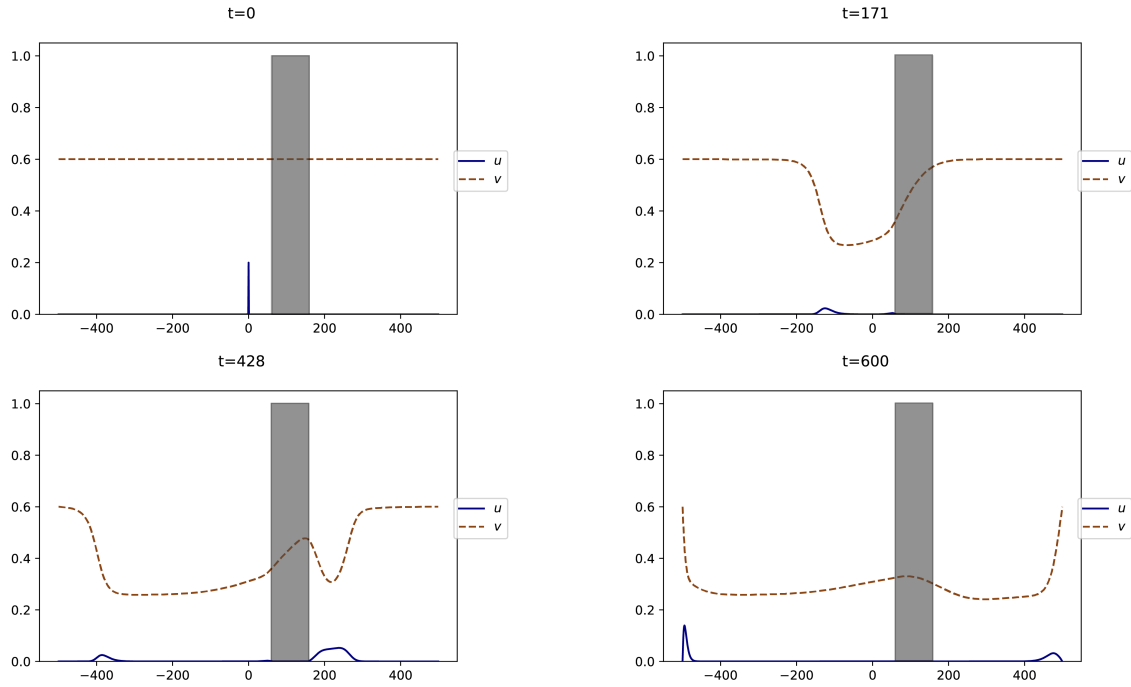


Figure 22: Gap problem – propagation. Snapshots at different times of the solution of (7.1) with $L = 100$, $v_b = 0.6$ and $u(x) = 0.2(1 - x^2)_+$. The shaded area represents the obstacle $\mathcal{K} = (60, 160)$. [Video: Gap_Hair-Trigger_inhibiting.mp4](#)

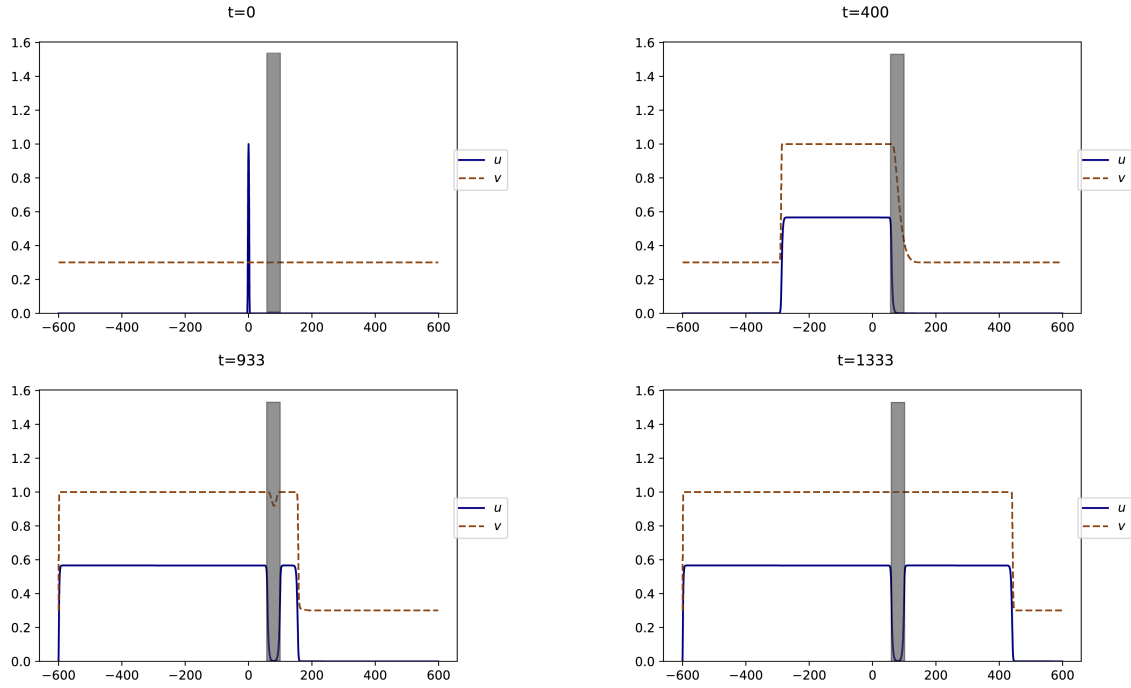


Figure 23: Gap problem – propagation. Snapshots at different times of the solution of (7.2) with $L = 40$, $v_b = 0.3$ and $u_0(x) = (1 - \frac{x^2}{10})_+$. The shaded area represents the obstacle $\mathcal{K} = (60, 100)$.
[Video: Gap=40.mp4](#)

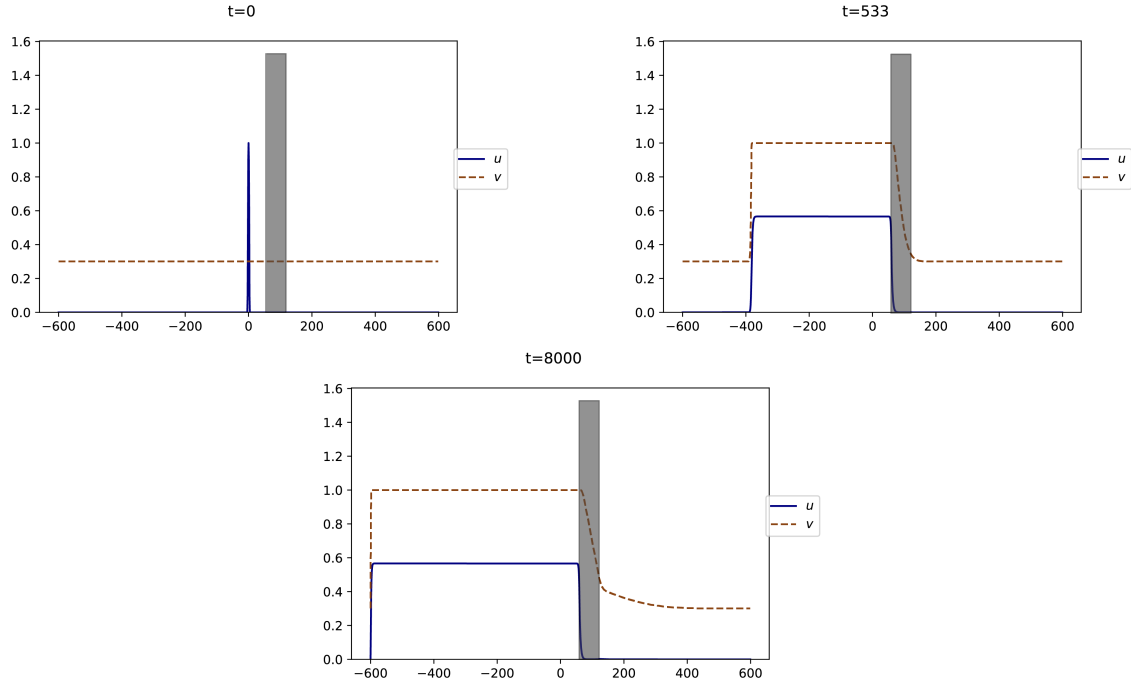


Figure 24: Gap problem – blockage. Snapshots at different times of the solution of (7.2) with $L = 60$, $v_b = 0.3$ and $u_0(x) = (1 - \frac{x^2}{10})_+$. Space is represented horizontally, and the shaded area represents the obstacle $\mathcal{K} = (60, 120)$. Blue solid line: $u(t, \cdot)$. Brown dashed line: $v(t, \cdot)$.
[Video: Gap=60.mp4](#)

vary between, for examples, cities and suburbs, or poor and rich areas (see [22]). To account for this situation with a model case, we may assume that $v_0(x) := v(t=0, x)$ is periodic and oscillates around the threshold v_* .

Consider the inhibiting system (4.5), that we recall here,

$$\begin{cases} \partial_t u - \partial_{xx} u = u \left[v(1-u) - \frac{1}{3} \right], \\ \partial_t v - \partial_{xx} v = -uv, \end{cases} \quad (7.3)$$

with $u_0(x) = 0.2(1-x^2)_+$ and

$$v_b(x) = \begin{cases} 0.2 & \text{if } |x| \in [100k, 100k+L], \\ 0.6 & \text{if } |x| \in (100k-L, 100k), \end{cases} \quad \forall k = 1, 2, \dots, \quad (7.4)$$

for some parameter $L \in (0, 100)$. We recall that, for equation (7.3), we have $v_* = \frac{1}{3}$ (where v_* is defined in (2.4)). Therefore, $v_0(x)$ oscillates periodically around v_* , creating zones of length $100-L$ that are favorable for propagation ($v_0(x) = 0.6 > v_*$), and zones of length L that are unfavorable ($v_0(x) = 0.2 < v_*$). If the favorable zone is sufficiently large, then the solution manages to propagate, as can be seen on Figure 25 for $L = 20$. On the contrary, if the favorable zone is too thin, then the propagation is blocked, as can be seen on Figure 26 for $L = 60$. (We point out that, for the numerical simulation, we impose $v_0(x) = 0.6$ on $(-60, 60)$ to ensure that the movement of social unrest gets properly ignited at $x = 0$ before being affected by the oscillations of v_b).

We leave for future works the rigorous analysis of the case of a non-constant initial level of social tension $v_0(\cdot) \equiv v_b(\cdot)$. In this case, however, let us indicate that the threshold phenomenon on the initial level of social tension may not involve the sign of $v_b - v_*$, but rather the sign of λ_b defined as the lowest eigenvalue of the operator, $\forall \varphi \in C^2(\Omega)$,

$$-d_1 \Delta \varphi - \partial_u \Phi(0, v_b(x)) \varphi,$$

and given by the expression

$$\lambda_b := \inf \left\{ \int_{\mathbb{R}^n} d_1 |\nabla \varphi|^2 - [r(v_b(x))f(0) - \omega] \varphi^2 : \varphi \in H^1(\mathbb{R}^n), \|\varphi\|_{L^2} = 1 \right\}.$$

7.3 Including geometry

Another possible way to include spatial heterogeneity in our model is to consider the system (2.3) on a domain $\Omega \subset \mathbb{R}^n$ rather than on the entire space. We may impose Neumann boundary condition

$$\partial_\nu u = 0, \quad \text{on } \partial\Omega,$$

with ∂_ν the outer normal derivative, accounting for the fact that there is no flux of individuals across the boundary.

From the modeling point of view, the boundary $\partial\Omega$ could stand for various structural spatial obstructions for rioters, such as streets, highways, fences, rivers, mountains etc. These features play sometimes a significant role; for example, the ring around Paris in the 2005 riots [22].

Mathematically speaking, it is known that heterogeneous geometry can largely affect the propagation properties of Reaction-Diffusion equations (e.g., see [13, 30]). However, fewer papers deal with systems of Reaction-Diffusion such as our system (2.3). We leave further investigations on this topic for future works.

8 Proofs

8.1 The tension inhibiting case

8.1.1 Traveling waves

Before proving the results from Section 4.1, we derive from (2.10) two general identities which will be useful in the following.

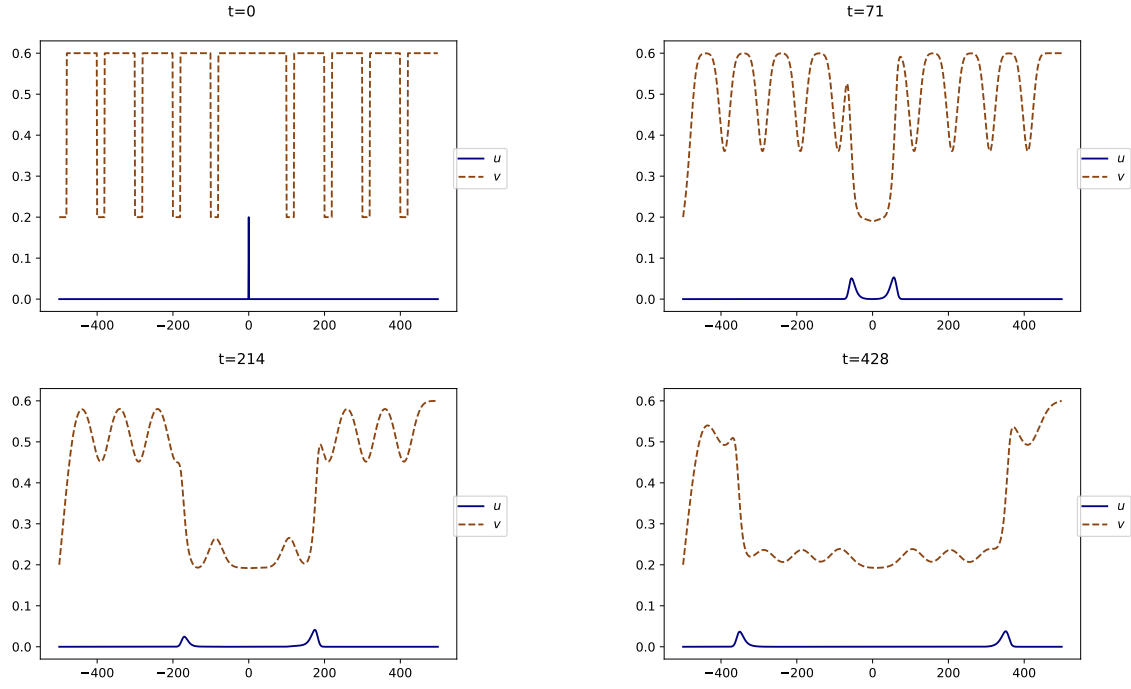


Figure 25: Non-uniform initial social tension v_0 – propagation. Snapshots at different times of the solution of (7.3)-(7.4) with $L = 20$, $u_0(x) = 0.2(1 - x^2)_+$. Horizontal axis: space. Blue solid line: $u(t, \cdot)$. Brown dashed line: $v(t, \cdot)$. [Video: Periodic_V0_L=20.mp4](#)

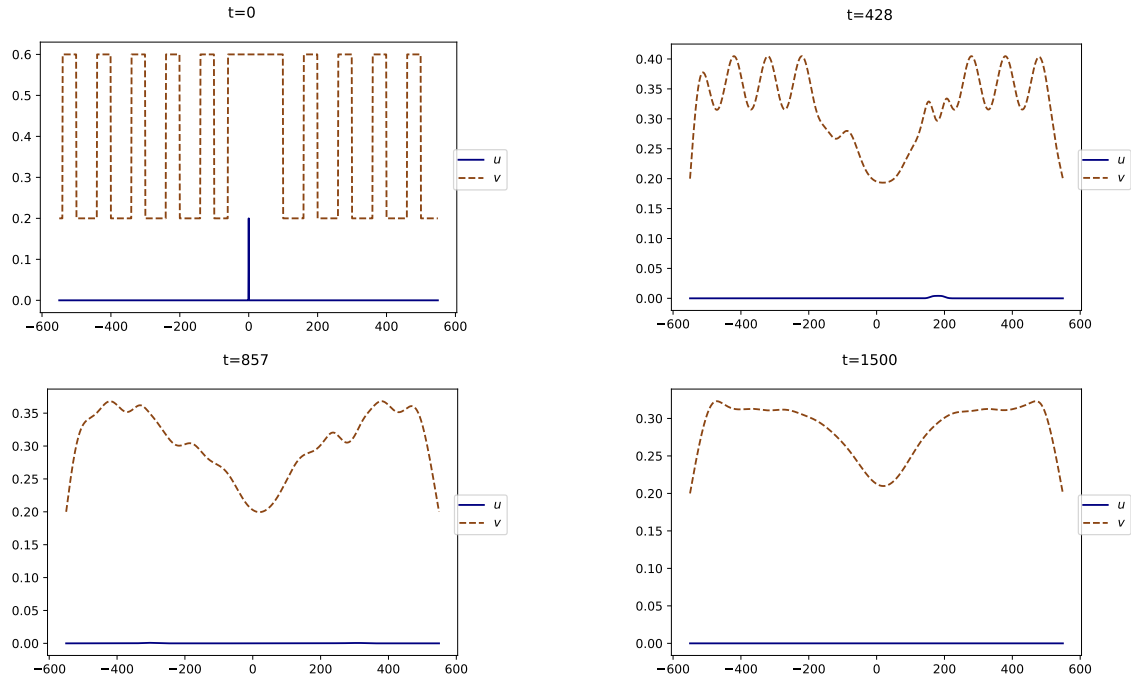


Figure 26: Non-uniform initial social tension v_0 – blockage. Snapshots at different times of the solution of (7.3)-(7.4) with $L = 60$, $u_0(x) = 0.2(1 - x^2)_+$. Horizontal axis: space. Blue solid line: $u(t, \cdot)$. Brown dashed line: $v(t, \cdot)$. [Video: Periodic_V0_L=60.mp4](#)

Lemma 8.1. Any solution U, V of (2.10) satisfies

$$U'(\xi) = \frac{1}{d_1} \int_{\xi}^{+\infty} e^{-\frac{c}{d_1}(z-\xi)} U(z) [r(V(z))f(U(z)) - \omega] dz, \quad (8.1)$$

and, if $d_2 > 0$,

$$V'(\xi) = \frac{1}{d_2} \int_{\xi}^{+\infty} e^{-\frac{c}{d_2}(z-\xi)} \Psi(U(z), V(z)) dz. \quad (8.2)$$

Proof. A straightforward computation gives

$$-\frac{d}{d\xi} \left(U'(\xi) e^{-\frac{c}{d_1}\xi} \right) = \frac{e^{-\frac{c}{d_1}\xi}}{d_1} \Phi(U, V).$$

Integrating this equation from ξ to $+\infty$ and using the boundedness of U' , which follows from elliptic estimates, we get (8.1). The proof of (8.2) is analogous. \square

Proof of Theorem 4.1. The inhibiting assumption (4.1) yields $\Psi(U, V) < 0$. If $d_2 = 0$, we directly deduce from (2.10) that $V' < 0$; the same conclusion holds when $d_2 > 0$ thanks to (8.2). Since V is also bounded, there holds that $V(+\infty) =: V_{\infty} \in [0, v_b]$.

Assume now by contradiction that $\limsup_{\xi \rightarrow +\infty} U(\xi) > 0$. Then, by the boundedness and uniform continuity of U (following from elliptic estimates) we can find $\varepsilon > 0$, $\delta > 0$ and a diverging sequence $(\xi_j)_{j \in \mathbb{N}}$ such that $U \geq \varepsilon$ in the interval $[\xi_j, \xi_j + \delta]$, for all $j \in \mathbb{N}$.

Suppose first that $V_{\infty} > 0$. In such case, (4.1) and (8.2) yield, for any $j \in \mathbb{N}$ and $\xi \in [\xi_j, \xi_j + \delta/2]$,

$$V'(\xi) \leq \frac{1}{d_2} \int_{\xi}^{\xi+\delta/2} e^{-\frac{c}{d_2}(z-\xi)} \Psi(U(z), V(z)) dz \leq \frac{1}{d_2} e^{-\frac{c\delta}{2d_2}} \min_{[\varepsilon, \sup U] \times [V_{\infty}, v_b]} \Psi < 0.$$

This, together with $V' \leq 0$, yields $V(+\infty) = -\infty$: a contradiction. Thus, $U(+\infty) = 0$ in such case.

Suppose now that $V_{\infty} = 0$. Since $r(0)f(0) < \omega$ by hypothesis (2.4), the monotonicity of f implies the existence of a constant $h > 0$ and $\bar{\xi} \in \mathbb{R}$ such that $r(V(\xi))f(U(\xi)) \leq r(V(\xi))f(0) \leq \omega - h$ for $\xi \geq \bar{\xi}$. Then (8.1) implies that $U' < 0$ in $(\bar{\xi}, +\infty)$ and moreover, for any $j \in \mathbb{N}$ such that $\xi_j \geq \bar{\xi}$ and $\xi \in [\xi_j, \xi_j + \delta/2]$,

$$U'(\xi) \leq \frac{1}{d_1} \int_{\xi}^{\xi+\delta/2} e^{-\frac{c}{d_1}(z-\xi)} U(z) [r(V(z))f(U(z)) - \omega] dz \leq -\frac{1}{d_1} e^{-\frac{c\delta}{2d_1}} \varepsilon h.$$

This leads to the contradiction $U(+\infty) = -\infty$. We have thereby shown that $U(+\infty) = 0$.

Since $U > 0$ and $U(+\infty) = 0$, there exists $\underline{\xi} \in \mathbb{R}$ such that $U'(\underline{\xi}) \leq 0$. Let us show that $U' \leq 0$ on $(\underline{\xi}, +\infty)$. By contradiction, assume that there exists $\bar{\xi} > \underline{\xi}$ such that $U'(\bar{\xi}) > 0$. By the continuity of U' and because $U(+\infty) = 0$, there exist $\xi \leq \xi_1 < \bar{\xi} < \xi_2$ such that $U' > 0$ in (ξ_1, ξ_2) and $U'(\xi_1) = U'(\xi_2) = 0$. Observe in particular that $U''(\xi_1) \geq 0$, whence, from the first equation in (2.10),

$$0 \geq U(\xi_1)(r(V(\xi_1))f(U(\xi_1)) - \omega).$$

By integrating the equation, and recalling that V is decreasing, this leads to the contradiction

$$c(U(\xi_2) - U(\xi_1)) = \int_{\xi_1}^{\xi_2} U(r(V)f(U) - \omega) < (\xi_2 - \xi_1)U(\xi_2)(r(V(\xi_1))f(U(\xi_1)) - \omega) \leq 0.$$

This means that the set where $U' \leq 0$ is given by some half-line $[\xi_0, +\infty)$.

Let us now show that the strict inequality $U' < 0$ holds in $(\xi_0, +\infty)$. Since U reaches its global maximum at ξ_0 , from the equation on U , we have

$$0 \leq -d_1 U''(\xi_0) = U(\xi_0)[r(V(\xi_0))f(U(\xi_0)) - \omega].$$

Differentiating the equation for U we get

$$c(U')' - d_1(U'')' = U'[r(V)f(U) - \omega] + Ur(V)f'(U)U' + Ur'(V)V'f(U).$$

The last term of the right-hand side is negative because $f(U) \geq f(U(\xi_0)) \geq \omega/r(V(\xi_0)) > 0$, which means that U' is a strict subsolution of a linear elliptic equation. Since U' is non positive in $(\xi_0, +\infty)$, the strong maximum principle implies that $U' < 0$ in $(\xi_0, +\infty)$.

It remains to show that V_∞ is a root of $\Psi(0, \cdot)$ and that $V_\infty \leq v_*$. The former property follows by observing that otherwise $\Psi(0, V_\infty) < 0$, due to (4.1), whence either (8.2) in the case $d_2 > 0$, or direct computation if $d_2 = 0$, would lead to the contradiction $\limsup_{\xi \rightarrow +\infty} V' < 0$. Instead, if $V_\infty > v_*$, then $r(V_\infty)f(0) > \omega$ and therefore (8.1) would imply that $U'(\xi) > 0$ for ξ large, contradicting what we have shown above. \square

Proof of Proposition 4.2. First of all, we know from Theorem 4.1 that $U(\pm\infty) = 0$, whence $U'(\pm\infty) = 0$ by elliptic estimates. From the equation on V , we get

$$U = \frac{cV'}{G(V)}.$$

Injecting this formula into the equation on U , and integrating over $(-\infty, +\infty)$ we find

$$c(U(+\infty) - U(-\infty)) = d_1(U'(+\infty) - U'(-\infty)) + c \int_{-\infty}^{+\infty} V' \left[\frac{r(V) - \omega}{G(V)} \right],$$

that is,

$$\int_{-\infty}^{+\infty} V' \left[\frac{r(V) - \omega}{G(V)} \right] = 0,$$

and so $Q(V_\infty) - Q(v_b) = 0$ \square

8.1.2 Large time behavior

Let us first give a proof of Proposition 4.4 which rests on elementary arguments.

Proof of Proposition 4.4. The smallness of u_0 is determined by the following condition:

$$\forall v \in [\tilde{v}_b, v_b], \quad r(v)f(u_0) > \omega, \quad (8.3)$$

which can be achieved since $v_b \geq \tilde{v}_b > v_*$ and so $r(v)f(0) > \omega$ for all $v \in [\tilde{v}_b, \tilde{v}]$. For all time $t \geq 0$, both $u(t, \cdot)$ and $v(t, \cdot)$ are constant. We thus omit to write the dependence on x . The proof relies on a simple argument in the phase plane. Denote $\gamma(t)$ and $\tilde{\gamma}(t)$ the trajectories in the plane (u, v) , namely $\gamma(t) := (u(t), v(t))$ and $\tilde{\gamma}(t) := (\tilde{u}(t), \tilde{v}(t))$. By the inhibiting assumption (4.1), these trajectories are nonincreasing in the v component and, by Theorem 4.3, they have two endpoints $(0, v_\infty)$, $(0, \tilde{v}_\infty)$ respectively. In addition, by uniqueness of solutions of the Cauchy problem, they cannot cross each other, nor can γ cross the segment $\{u_0\} \times (\tilde{v}_b, v_b)$, because there $u' > 0$ thanks to (8.3). The result then follows. \square

Let us now turn to the more intricate proof of Theorem 4.3. In the proof, we use the following result quoted from [17].

Lemma 8.2. [17, Theorem 5] *Under the inhibiting assumption (4.1), the solution (u, v) is bounded.*

Proof of the first statement of Theorem 4.3. Let us suppose for the moment that

$$\inf_{t>0} v(t, 0) > 0. \quad (8.4)$$

We claim the following:

$$\forall \varepsilon > 0, \exists \tau > 0, \quad \min_{t \in [t_0, t_0 + \tau]} u(t, 0) < \varepsilon, \quad \text{for all } t_0 \geq 0. \quad (8.5)$$

This would imply that $u(t, 0) \rightarrow 0$ along some diverging sequence of t , and therefore property (4.3) thanks to the parabolic Harnack inequality, c.f. [8, Theorem 3].

Assume by contradiction that the claim (8.5) does not hold, that is, there exists $\varepsilon > 0$ such that, for any $\tau > 0$, we can find $t_\tau > 0$ so that $u(t, 0) \geq \varepsilon$ for all $t \in [t_\tau, t_\tau + \tau]$. Observe that u and v , being bounded owing to Lemma 8.2, are uniformly continuous by parabolic estimates. Thus, by the contradictory assumption and (8.4), we can find $\delta > 0$ such that

$$\inf_{\substack{t \in [t_\tau, t_\tau + \tau] \\ x \in B_\delta}} u(t, x) > \varepsilon/2, \quad \inf_{\substack{t > 0 \\ x \in B_\delta}} v(t, x) > 0,$$

where B_δ is the ball centered at $x = 0$ of radius δ . As a consequence, owing to (4.1), the function

$$\tilde{\Psi}(t, x) := \frac{\Psi(u(t, x), v(t, x))}{u(t, x)},$$

satisfies

$$\tilde{\Psi} < 0 \quad \text{in } \mathbb{R} \quad \text{and} \quad m := \sup_{\substack{t \in [t_\tau, t_\tau + \tau], \\ x \in B_\delta}} \tilde{\Psi}(t, x) < 0. \quad (8.6)$$

Let us set $w(t, x) := v(t, x) - v_b$. This is a solution of the equation

$$w_t - d_2 \Delta w = \tilde{\Psi}(t, x)u, \quad t > 0, \quad x \in \mathbb{R}^n,$$

with initial condition $w(0, x) \equiv 0$. We can explicitly compute w using the heat kernel:

$$w(t, x) = \int_\tau^t \frac{1}{(4\pi d_2(t-s))^{n/2}} \int_{\mathbb{R}^n} e^{-\frac{|x-y|^2}{4\pi d_2(t-s)}} \tilde{\Psi}(s, y) u(s, y) dy ds.$$

It follows from (8.6) that

$$\begin{aligned} w(t_\tau + \tau, x_0) &\leq m \frac{\varepsilon}{2} \int_{t_\tau}^{t_\tau + \tau - 1} \frac{1}{(4\pi d_2(t_\tau + \tau - s))^{n/2}} \int_{B_\delta} e^{-\frac{|x-y|^2}{4\pi d_2(t_\tau + \tau - s)}} dy ds \\ &\leq m \frac{\varepsilon}{2} e^{-\frac{\delta^2}{2\pi d_2}} |B_\delta| \int_0^{\tau-1} \frac{1}{(4\pi d_2(\tau - s))^{n/2}} ds. \end{aligned}$$

Observe that the last term tends to $-\infty$ as $\tau \rightarrow +\infty$ provided $n \leq 2$. This means that $\inf v = -\infty$, which is impossible because $v \geq 0$. Whence (8.5) holds, which concludes the proof provided v satisfies (8.4).

Next, if (8.4) does not hold then $v(t_k, 0) \rightarrow 0$ as $k \rightarrow +\infty$ for some sequence $(t_k)_{k \in \mathbb{N}}$ diverging to $+\infty$. By parabolic estimates and the boundedness provided by Lemma 8.2, the sequences of functions $u(t + t_k, x)$, $v(t + t_k, x)$ converge locally uniformly (up to subsequences) as $k \rightarrow +\infty$ to some functions $\tilde{u}(t, x)$, $\tilde{v}(t, x)$ respectively, solutions in $t \in \mathbb{R}$, $x \in \mathbb{R}^n$ of

$$\begin{cases} \partial_t \tilde{u} - d_1 \Delta \tilde{u} = \tilde{u} [r(\tilde{v})f(\tilde{u}) - \omega], \\ \partial_t \tilde{v} - d_2 \Delta \tilde{v} = \Psi(\tilde{u}, \tilde{v}), \end{cases}$$

with $\tilde{v} \geq 0$ and vanishing at $(0, 0)$. The strong maximum principle then yields $\tilde{v} \equiv 0$ (recall that $\Psi(\cdot, 0) = 0$ by (2.6) and (4.1)). This, in turn, yields

$$\partial_t \tilde{u} - d_1 \Delta \tilde{u} = \tilde{u} [r(0)f(\tilde{u}) - \omega] \leq \tilde{u} [r(0)f(0) - \omega].$$

Recalling that $r(0)f(0) < \omega$ by assumption (2.4), one readily deduces from the boundedness of \tilde{u} that $\tilde{u} \equiv 0$, whence (4.3) holds. \square

In order to prove the second statement of Theorem 4.3, we make use of the following classical lemma, whose proof is inspired from that of [12, Theorem 1.8].

Lemma 8.3. *Let $w \in C^2(\mathbb{R}^n)$ be a bounded function satisfying $w \Delta w \geq 0$ in \mathbb{R}^n . If $n \leq 2$, then w is constant.*

Proof. For $R > 0$, we define a cut-off function

$$\chi_R(x) := \chi \left(\frac{|x|}{R} \right), \quad \forall x \in \mathbb{R}^n,$$

for χ a smooth nonnegative function such that

$$\chi(z) = \begin{cases} 1 & \text{if } 0 \leq z \leq 1, \\ 0 & \text{if } z \geq 2, \end{cases} \quad |\chi'| \leq 2.$$

Multiplying the equation on w by χ_R^2 , integrating on \mathbb{R}^n and using the divergence theorem, we find

$$\begin{aligned} 0 &\leq - \int_{\mathbb{R}^n} \nabla (\chi_R^2 w) \cdot \nabla w \\ &= - \int_{\mathbb{R}^n} \chi_R^2 |\nabla w|^2 - 2 \int_{\mathbb{R}^n} \chi_R w \nabla \chi_R \cdot \nabla w. \end{aligned}$$

Using the Cauchy-Schwarz inequality, we deduce

$$\int_{\mathbb{R}^n} \chi_R^2 |\nabla w|^2 \leq 2 \sqrt{\int_{B_{2R} \setminus B_R} \chi_R^2 |\nabla w|^2} \sqrt{\int_{\mathbb{R}^n} w^2 |\nabla \chi_R|^2}, \quad (8.7)$$

where B_R is the ball of radius R and center 0. Recall that w is bounded and that $|\nabla \chi_R|^2 \leq R^{-2} \|\nabla \chi\|_\infty$. As $n \leq 2$, we deduce that

$$\int_{\mathbb{R}^n} w^2 |\nabla \chi_R|^2 \text{ is bounded, uniformly in } R \geq 1.$$

From (8.7), we have that $\int_{\mathbb{R}^n} \chi_R^2 |\nabla w|^2$ is uniformly bounded. Therefore, $\int_{B_{2R} \setminus B_R} \chi_R^2 |\nabla w|^2$ converges to 0 as $R \rightarrow +\infty$, and so the term on the left-hand side of (8.7) also converges to 0. At the limit, we find $\int_{\mathbb{R}^n} |\nabla w|^2 \leq 0$. Hence $\nabla w \equiv 0$, which ends the proof. \square

Proof of the second statement of Theorem 4.3. Assume that $v(t, x)$ converges pointwise to some $v_\infty(x)$ as $t \rightarrow +\infty$. From classical parabolic estimates, the convergence actually occurs in C_{loc}^2 . Since $\partial_t v - \Delta v \leq 0$, when $t \rightarrow +\infty$ we find

$$-\Delta v_\infty \leq 0 \quad \text{on } \mathbb{R}^n.$$

Lemma 8.3 implies that v_∞ is constant.

We claim that $v_\infty \leq v_\star$. By contradiction, assume $v_\infty > v_\star$, then, for t large enough, u satisfies

$$\partial_t u \geq d_1 \Delta u + u(r(\alpha)f(u) - \omega),$$

with $\alpha := \frac{v_\infty + v_\star}{2} > v_\star$. Thus, u is a supersolution of a classical KPP equation, we deduce

$$\liminf_{t \rightarrow +\infty} u(t, x) > 0.$$

We reach a contradiction with the first assertion of Theorem 5.2, namely (4.3), which we proved previously.

Finally, let us show that $u(t, \cdot)$ converges locally uniformly to 0 when $t \rightarrow +\infty$. Let us first consider the case $v_\infty \neq 0$. By contradiction, assume that there exists a diverging sequence of times $t_k > 0$ and a ball $B \subset \mathbb{R}^n$ such that

$$\inf_{\substack{k \geq 0 \\ x \in B}} u(t_k, x) > 0. \quad (8.8)$$

We use the notation

$$\tilde{\Psi}(t, x) := \frac{\Psi(u, v)}{u}.$$

Since $v_\infty \in (0, 1)$, the inhibiting assumption (4.1) implies

$$\sup_{\substack{k \geq 0 \\ x \in B}} \tilde{\Psi}(t_k, x) < 0. \quad (8.9)$$

From the equation on v , we can write

$$\partial_t v - \Delta v = u \tilde{\Psi}.$$

From the convergence of $v(t, \cdot)$, we deduce that $u(t, \cdot) \tilde{\Psi}(t, \cdot)$ converges locally uniformly to 0 as $t \rightarrow +\infty$. From (8.9), we thus have that $u(t_k, x)$ converges to 0 as $k \rightarrow +\infty$ and $x \in B$: we reach a contradiction with (8.8).

Let us now consider the case $v_\infty = 0$. Fixing $\varepsilon \in (0, v_\star)$, for t large enough u satisfies

$$\partial_t u - d_1 \Delta u \leq u(r(\varepsilon)f(u) - \omega) \leq -Cu,$$

where $C := \omega - r(\varepsilon)f(0) > 0$. It proves that $u(t, \cdot)$ converges uniformly to 0 as $t \rightarrow +\infty$. \square

8.2 The tension enhancing case

Proof of Theorem 5.1. We first show that the enhancing assumption (5.1) yields $U < M$. Observe that if U has a local maximum at some point $\tilde{\xi}$ then the first equation in (2.10) implies that

$$r(V(\tilde{\xi}))f(U(\tilde{\xi})) \geq \omega,$$

whence $U(\tilde{\xi}) < M$ by (5.1). It follows that if $U(\tilde{\xi}) = M$ at some $\tilde{\xi} \in \mathbb{R}$, then necessarily $U' \geq 0$ on $[\tilde{\xi}, +\infty)$, and moreover $U(+\infty) > M$. But then (8.1) from Lemma 8.1, together with (5.1), yield

$$U'(\tilde{\xi}) = \frac{1}{d_1} \int_{\tilde{\xi}}^{+\infty} e^{-\frac{c}{d_1}(z-\tilde{\xi})} U(z) [r(V(z))f(U(z)) - \omega] dz < 0,$$

hence a contradiction.

Next, we show that $V' > 0$. Assumption (5.1) yields $\Psi(U, V) > 0$. If $d_2 = 0$, we directly deduce from (2.10) that $V' > 0$; the same conclusion holds when $d_2 > 0$ thanks to (8.2).

Let us show that $U' \geq 0$. By contradiction, assume that $U'(\tilde{\xi}) < 0$ at some $\tilde{\xi} \in \mathbb{R}$. Hence, because $U(-\infty) = 0$, there exist $\xi_1 < \tilde{\xi} < \xi_2 \leq +\infty$ such that $U' < 0$ in (ξ_1, ξ_2) and $U'(\xi_1) = U'(\xi_2) = 0$. Observe in particular that $U''(\xi_1) \leq 0$, whence, from the first equation in (2.10),

$$0 \leq U(\xi_1)(r(V(\xi_1))f(U(\xi_1)) - \omega).$$

By integrating the equation, this leads to the contradiction

$$c(U(\xi_2) - U(\xi_1)) = \int_{\xi_1}^{\xi_2} U(r(V)f(U) - \omega) > (\xi_2 - \xi_1)U(\xi_2)(r(V(\xi_1))f(U(\xi_1)) - \omega) \geq 0.$$

Hence $U' \geq 0$.

Now that we know that both $U(+\infty)$ and $V(+\infty)$ exist, we readily deduce from (8.1) and (8.2) the following equivalences, respectively:

$$r(V(+\infty))f(U(+\infty)) = \omega, \quad \Psi(U(+\infty), V(+\infty)) = 0.$$

Recalling that $U(+\infty) \in (0, M]$ and $V(+\infty) \in (0, 1]$, owing to (5.1) we infer from the first equivalence that $U(+\infty) < M$ and thus from the second one that $V(+\infty) = 1$, which in turn yields $r(1)f(U(+\infty)) = \omega$.

To conclude the proof it remains to show the strict inequality $U' > 0$. Differentiating the equation for U we get

$$c(U')' - d_1(U'') = U'[r(V)f(U) - \omega] + Ur(V)f'(U)U' + Ur'(V)V'f(U)U.$$

The last term of the right-hand side is positive because $f(U) \geq f(U(+\infty)) = \omega/r(1) > 0$, which means that U' is a nonnegative strict supersolution of a linear elliptic equation. This prevents U' from vanishing. \square

Proof of Theorem 5.2 in the case $d_2 > 0$. First of all, we know from Lemma 2.1 that $u > 0$ and $0 < v < 1$ for all $t > 0$, $x \in \mathbb{R}^n$. The proof is achieved in four steps: we first derive an upper bound for u , next a lower bound for v , then for u , and we finally conclude.

Upper bound for u .

Let us derive the upper bound for u as $t \rightarrow +\infty$. We see that, by the monotonicity of r ,

$$\partial_t u - d_1 \Delta u \leq u[r(1)f_+(u) - \omega],$$

where $f_+ := \max\{f, 0\}$ is the positive part of f . Let U be the solution of the ODE $U' = U(r(1)f_+(U) - \omega)$ with initial datum $U(0) = \max\{M, \sup u_0\}$. There holds that $U \searrow u_\star(1)$ given by (2.9), i.e., the zero of $u \mapsto r(1)f(u) - \omega$, whose existence and uniqueness is guaranteed by (2.4) and (5.1). Then, by comparison, we get the desired upper bound:

$$\limsup_{t \rightarrow +\infty} \left(\sup_{x \in \mathbb{R}^n} u(t, x) \right) \leq u_\star(1) < M.$$

It follows that there exist $M' < M$ and $T > 0$ such that

$$u(t, x) \leq M' < M, \quad \forall t \geq T, x \in \mathbb{R}^n. \quad (8.10)$$

Lower bound for v .

Consider a sequence $(x_k)_{k \in \mathbb{N}}$ in \mathbb{R}^n such that $|x_k| \rightarrow +\infty$. By parabolic estimates, the functions $u(\cdot, x_k + \cdot)$, $v(\cdot, x_k + \cdot)$ converge (up to subsequences) as $k \rightarrow +\infty$, locally uniformly in $[0, +\infty) \times \mathbb{R}^n$, to some functions \tilde{u} , \tilde{v} which are still solutions of (2.3), with initial datum $(0, v_b)$. Hence $(\tilde{u}, \tilde{v}) \equiv (0, v_b)$ because $\Phi(0, v_b) = \Psi(0, v_b) = 0$. This means that $(u(t, x), v(t, x)) \rightarrow (0, v_b)$ as $|x| \rightarrow +\infty$, for any given $t \geq 0$. In particular, for any fixed $t \geq 0$ and $\underline{v} \in (v_*, v_b)$, we have that $v(t, x) > \underline{v}$ for $|x|$ sufficiently large. Moreover, (5.1) and (8.10) imply that $\Psi(u, v) > 0$ for $t \geq T$, $x \in \mathbb{R}^n$, that is, v is a supersolution of the heat equation, and we know that at time T it is larger than \underline{v} outside a large ball. By comparison with the heat equation, one readily deduces that, for given $\underline{v}' \in (v_*, \underline{v})$, there exists $T' > T$ such that

$$v(t, x) \geq \underline{v}' > v_*, \quad \forall t \geq T', \quad x \in \mathbb{R}^n. \quad (8.11)$$

Lower bound for u .

Consider the equation

$$\partial_t \hat{u} - d_1 \Delta \hat{u} = \hat{u} [r(\underline{v}') f(\hat{u}) - \omega],$$

which is a standard scalar KPP equation. Observe indeed that $r(\underline{v}') f(0) - \omega > 0 > r(\underline{v}') f(M) - \omega$ by the definition (2.4) of v_* and (5.1). We consider the solution of this KPP equation starting at time T' with the datum $\hat{u}(T', x) = \min\{u(T', x), u_*(\underline{v}')\}$, where $u_*(\underline{v}') > 0$ is given by (2.9), i.e., $r(\underline{v}') f(u_*(\underline{v}')) = \omega$. It follows from the classical result of [7] that $\hat{u}(t, x) \nearrow u_*(\underline{v}')$ as $t \rightarrow +\infty$, locally uniformly in $x \in \mathbb{R}^n$. For $t \geq T'$, using that $\hat{u}(t, \cdot) \leq u_*(\underline{v}')$ and $v(t, \cdot) \geq \underline{v}'$ by (8.11), we see that \hat{u} is a subsolution of the first equation in (2.3), whence, by comparison,

$$\liminf_{t \rightarrow +\infty} u(t, x) \geq u_*(\underline{v}'), \quad \forall x \in \mathbb{R}^n. \quad (8.12)$$

Conclusion.

Let $(t_k)_{k \in \mathbb{N}}$ be an arbitrary sequence diverging to $+\infty$. The functions $u(t_k + \cdot, \cdot)$, $v(t_k + \cdot, \cdot)$ converge (up to subsequences) as $k \rightarrow +\infty$, locally uniformly in $\mathbb{R} \times \mathbb{R}^n$, to some functions u_∞ , v_∞ which are entire solutions (i.e., for $t \in \mathbb{R}$, $x \in \mathbb{R}^n$) of the equations in (2.3). Moreover, (8.10), (8.11), (8.12) yield $u_*(\underline{v}') \leq u_\infty \leq u_*(1)$ and $v_\infty \geq \underline{v}'$. From (5.1) we deduce that necessarily $v_\infty \equiv 1$ and then that $u_\infty \equiv u_*(1)$. \square

Proof of Theorem 5.2 in the case $d_2 = 0$. We immediately see that $0 < u < \max\{\sup u_0, M\}$, owing to (5.1) and the parabolic strong maximum principle, and that $0 < v < 1$, by elementary ODE considerations, for all $t > 0$, $x \in \mathbb{R}^n$. Moreover, we observe that the upper bound (8.10) for u is derived in the above proof for the case $d_2 > 0$ only by arguing on the first equation in (2.3), hence it holds true when $d_2 = 0$. We want to derive now the upper bound

$$u(t, x) < M, \quad \forall t \geq 0, \quad |x| \geq R, \quad (8.13)$$

for some possibly very large R . For this we consider, for any given direction $e \in \mathbb{S}^{n-1}$, the function

$$u_e(t, x) = e^{\sigma(t+1) - x \cdot e}.$$

It is readily seen that there exists σ sufficiently large so that this is a supersolution of the first equation in (2.3). Moreover, since u_0 is compactly supported, we can choose σ , possibly even larger and independent of e , so that in addition $u_e(0, x) > u_0(x)$ for all $x \in \mathbb{R}^n$. Therefore, by comparison, $u \leq u_e$ for all $t \geq 0$ and $x \in \mathbb{R}^n$, which, being true for any $e \in \mathbb{S}^{n-1}$, yields $u(t, x) \leq e^{\sigma(t+1) - |x|}$. We deduce in particular that $u(t, x) < M$ for all $t \in [0, T]$ and $|x| \geq \sigma(T+1) - \log M$. Combining this with (8.10) eventually gives (8.13) with $R = \sigma(T+1) - \log M$.

We now use the upper bound (8.13) for u in the equation for v . Owing to (5.1), it implies that, for $t \geq 0$ and $|x| \geq R$, $\partial_t v = \Psi(u, v) > 0$, hence

$$v(t, x) \geq v_b, \quad \forall t \geq 0, \quad |x| \geq R. \quad (8.14)$$

Let us derive a lower bound on u . Let λ_ρ be the Dirichlet principal eigenvalue of $-\Delta$ in B_ρ , and φ_ρ be the associated (positive) eigenfunction. It is well known that $\lambda_\rho \searrow 0$ as $\rho \rightarrow +\infty$, hence in particular $d_1 \lambda_\rho < r(v_b) f(0) - \omega$ for ρ large enough, because $v_b > v_*$ defined by (2.4) and therefore $r(v_b) f(0) > \omega$. It follows that, for such a ρ and for $\varepsilon > 0$ small enough,

$$-d_1 \Delta(\varepsilon \varphi_\rho) = \lambda_\rho \varepsilon \varphi_\rho < \varepsilon \varphi_\rho [r(v_b) f(\varepsilon \varphi_\rho) - \omega],$$

whence, by (8.14), $\varepsilon\varphi_\rho(x-x_0)$ is a subsolution to the first equation in (2.3) for $t > 0$ and $x \in B_\rho(x_0)$ whenever $|x_0| > R + \rho$. Take x_0 satisfying $|x_0| > R + \rho$ and $\varepsilon > 0$ small enough so that the above property holds and moreover $\varepsilon\varphi_\rho(x-x_0) < u(1, x)$ for all $x \in B_\rho(x_0)$. The comparison principle yields $u(t, x) > \varepsilon\varphi_\rho(x-x_0)$ for all $t \geq 1$, $x \in B_\rho(x_0)$, thus, using the parabolic Harnack inequality, we find, for any compact set $\mathcal{K} \subset \mathbb{R}^n$,

$$m := \inf_{\substack{t \geq 2 \\ x \in \mathcal{K}}} u(t, x) > 0. \quad (8.15)$$

We are now in a position to conclude. For $s \geq 0$ call

$$g(s) := \min_{z \in [m, M']} \Psi(z, s).$$

This function satisfies $g(s) > 0$ for $s \in (0, 1)$ by (5.1) and $g(1) = 0$ by (2.6). For $t \geq \max\{T, 2\}$ and $x \in \mathcal{K}$, since $m \leq u(t, x) \leq M'$ by (8.10) and (8.15), we see that

$$\partial_t v(t, x) = \Psi(u, v) \geq g(v).$$

As a consequence, because $\min_{x \in \mathcal{K}} v(\max\{T, 2\}, x) > 0$, by the continuity of v , we infer that $v(t, x) \rightarrow 1$ as $t \rightarrow +\infty$ uniformly in $x \in \mathcal{K}$. We have thereby shown that $v(t, x) \rightarrow 1$ as $t \rightarrow +\infty$ locally uniformly in $x \in \mathbb{R}^n$. Finally, for any sequence $(t_k)_{k \in \mathbb{N}}$ diverging to $+\infty$, the function $u(t_k + \cdot, \cdot)$ converges (up to subsequences) as $k \rightarrow +\infty$, locally uniformly in $\mathbb{R} \times \mathbb{R}^n$, to a nonnegative, bounded solution \tilde{u} of

$$\partial_t \tilde{u} - d_1 \Delta \tilde{u} = \tilde{u} [r(1)f(\tilde{u}) - \omega],$$

which satisfies $\tilde{u}(t, x) \geq m$ for all $t \in \mathbb{R}$, $x \in \mathcal{K}$ thanks to (8.15). It is a straightforward consequence of [7] that the only entire solution of this standard KPP equation satisfying such a property is $\tilde{u} \equiv u_\star(1)$. This concludes the proof. \square

9 Conclusion

9.1 Main findings

An increasing number of papers consider systems of Reaction-Diffusion equations to model the dynamics of riots or other collective behaviors. However, most of the work study particular and different cases. In this paper, we try to propose a unified mathematical approach, based on the theoretical framework developed in [17]. Although we focus on the problem of modeling social unrest, our goal is to keep a rather general mathematical approach that can be transposed to other topics in social dynamics.

Our model involves two quantities, the level social unrest u and the level of social tension v , which play asymmetric roles. We examine the problem of a system initially at equilibrium $u = 0$, $v = v_b$, for which a triggering event $u_0(\cdot) \geq 0$ occurs at $t = 0$. After stating our modeling assumptions, we derive the Reaction-Diffusion system (2.3).

In Section 3, we highlight a threshold phenomenon on the initial level of social tension $v_0 \equiv v_b$. On the one hand, if v_b is below a threshold value v_\star and the triggering event is small enough, the system returns to equilibrium quickly, and we speak of a return to calm. On the other hand, if v_b is above v_\star , an arbitrarily small triggering event causes an eruption of social unrest. Then, the movement of social unrest spreads through space with an asymptotically constant speed.

The core of the paper deals with two classes of models, for which we are able to derive more complete theoretical and numerical results.

The first one, called *tension inhibiting*, is such that the movement of social unrest dissipates social tension. Once the level of social tension falls below the threshold value v_\star , in turn, the level of social unrest fades until it is extinguished as $t \rightarrow +\infty$. This behavior is exhibited by both traveling wave solutions, c.f. Theorem 4.1, as well as by solutions of the Cauchy problem, c.f. Theorem 4.3. Tension inhibiting models thus give rise to limited duration movement of social agitation, that we call “riots”. An interesting property is that the intensity of the triggering event has no influence on the qualitative dynamic of the system. We numerically observe that the solution converges to two opposite traveling waves moving with the speed $c_b := 2\sqrt{r(v_b)f(0) - \omega}$ (which does not

depend on the parameters of the equation on v) and link the steady state $(0, v_b)$ to another one $(0, v_\infty)$, the profile of u having the shape of a bump, and that of v a monotonous decreasing wave, linking . We also investigate theoretically and numerically the question of estimating the final level of social tension v_∞ , revealing the non-monotonic structure underlying the inhibiting system, see Proposition 4.4.

The second specific class of models we examine is the *tension enhancing*. For such systems, if the initial level of social tension v_b is higher than the threshold value v_\star , the dynamics gives rise to a movement of social agitation that converges in a long time to a sustainable excited state. This case typically accounts for time-persisting social movements, which we call here lasting upheaval. We numerically observe that if $v_b < v_\star$, the solution converges towards two opposite traveling waves, whose speed can take intermediate values between c_b and $c_1 := 2\sqrt{r(1)f(1)} - \omega$ (depending on the parameters of the equation on v , c.f. Figure 14). These waves connect $(0, v_b)$ to $(u_\star(1), 1)$ (from definition (2.9)), the profiles of u and v having the shape of increasing waves, c.f. Theorem 5.1. If $v_b < v_\star$, contrarily to the *tension inhibiting* case, we observe that a sufficiently strong triggering event can still ignite a lasting upheaval, see Figure 11.

The *tension inhibiting* and *tension enhancing* classes of models give a good idea of the variety of behaviors that our model can generate. In Section 6, we examine mixed cases that exhibit more complex behaviors; some models feature a double threshold effect between *return to calm*, *riot* and *lasting upheaval*, others generate oscillating traveling waves or terraces (consisting of a riot followed by a lasting upheaval).

In Section 7, we propose several ways to include spatial heterogeneity in our model. We first consider the case of heterogeneous coefficients and study how an obstacle (i.e. an area of depressed growth for social unrest) affects the propagation of a social movement. On the one hand, if $v_b > v_\star$, the propagation of the social movement is guaranteed in any case. On the other hand, if $v_b < v_\star$, propagation is only possible if the triggering event is sufficiently large and the gap is sufficiently small. We then consider the case of an initial level of social tension v_0 that is not constant. This case accounts for the variability of populations according to the neighborhood (for example, between a city and its suburbs) which may have a significant impact on social movement according to data. Finally, we mention that our framework allows to include geometrical heterogeneity through the domain on which we pose the system of equations (2.3).

9.2 Possible extensions and perspectives

We conclude by mentioning several other extensions which are relevant regarding the modeling of social unrest.

9.2.1 Non-local diffusion

A possible extension of our model is to replace the Laplace operator in (2.3) with some non-local diffusion operator. One can consider, for example, that the classical diffusion is replaced by the convolution with an integrable kernel $K(\cdot)$

$$K * u(x) = \int_{\Omega} K(x - y)u(y)dy.$$

Another interesting example is the fractional Laplacian, for $s \in (0, 1)$,

$$\Delta^s u(x) = c_{n,s} \int_{\mathbb{R}^n} \frac{u(x) - u(y)}{|x - y|^{n+2s}} dy, \quad \forall x \in \mathbb{R}^n,$$

with $c_{n,s}$ a normalization constant.

On the one hand, a non-local diffusion on the level of activity u could account for the fact that rioters can travel to another location. On the other hand, a nonlocal on the level of social tension could account for the global spreading of information through media.

Non-local diffusion is increasingly used in various modeling situations (e.g., [18] deals with the modeling of riots, and [57] contains many other topics), and often leads to some anomalous behaviors. We let the reader refer to [53, 57] and references therein for more details.

9.2.2 Compartmental models

An underlying hypothesis of our modeling approach is that all individuals are identical. Yet, the variability of individuals sometimes plays an important role in collective behaviors [38, 42]. It is often admitted that certain social and economic classes are more prone to trigger or drive a social movement, such as students [2], rural population [63], activists [59], etc.

One way to include individuals variability in our model is to consider two different levels of activity u_1 and u_2 , the first accounting for the rioting activity of activist and leaders, the other accounting for the rioting activity of more reluctant individuals. It remains unclear how our conclusions would be affected by this additional feature, and we leave this question as an open problem.

Acknowledgments

The research leading to these results has received funding from the European Research Council under the European Union's Seventh Framework Programme (FP/2007-2013) / ERC Grant Agreement n. 321186 - ReaDi - "Reaction-Diffusion Equations, Propagation and modeling" held by Henri Berestycki. This work was also partially supported by the French National Research Agency (ANR), within project NONLOCAL ANR-14-CE25-0013.

References

- [1] K. Afassinou. Analysis of the impact of education rate on the rumor spreading mechanism. *Physica A*, 414:43–52, 2014.
- [2] P. G. Altbach and M. Klemencic. Student activism remains a potent force worldwide. *International Higher Education*, 76(2-3), 2014.
- [3] an Huo and N. Song. Dynamical interplay between the dissemination of scientific knowledge and rumor spreading in emergency. *Physica A*, 461:73–84, 2016.
- [4] an Huo, L. Wang, N. Song, C. Ma, and B. He. Rumor spreading model considering the activity of spreaders in the homogeneous network. *Physica A*, 468:855–865, 2017.
- [5] R. M. Anderson, editor. *The Population Dynamics of Infectious Diseases: Theory and Applications*. Springer US, Boston, MA, 1982.
- [6] H. Arendt. *Crises of the Republic : Lying in politics ; Civil disobedience ; On violence ; Thoughts on politics and revolution*. Harcourt Brace Jovanovich, 1972.
- [7] D. Aronson and H. Weinberger. Multidimensional nonlinear diffusion arising in population genetics. *Advances in Mathematics*, 30(1):33–76, oct 1978.
- [8] D. G. Aronson and J. Serrin. Local behavior of solutions of quasilinear parabolic equations. *Archive for Rational Mechanics and Analysis*, 25:81–122, 1967.
- [9] M. Bages and P. Martinez. Existence of pulsating waves in a monostable reaction-diffusion system in solid combustion. *Discrete and Continuous Dynamical Systems - Series B*, 14(3):817–869, 2010.
- [10] N. T. J. Bailey. *The mathematical theory of infectious diseases and its applications*. Griffin, London, 2nd edition, 1975.
- [11] P. Baudains, A. Braithwaite, and S. D. Johnson. Spatial Patterns in the 2011 London Riots. *Policing*, 7(1):21–31, mar 2013.
- [12] H. Berestycki, L. Caffarelli, and L. Nirenberg. Further qualitative properties for elliptic equations in unbounded domains. *Annali della Scuola Normale Superiore di Pisa, Classe di Scienze 4e série*, 25(1-2):69–94, 1997.
- [13] H. Berestycki, F. Hamel, and H. Matano. Bistable travelling waves around an obstacle. *Communications in Pure and Applied Mathematics*, 62(6):729–788, 2009.

- [14] H. Berestycki and B. Larrouturou. *Quelques aspects mathématiques de la propagation des flammes prémélangées*, volume X. Pitman, London, 1991.
- [15] H. Berestycki, J.-P. Nadal, and N. Rodríguez. A model of riot dynamics: shocks, diffusion, and thresholds. *Networks and Heterogeneous Media*, 10(3):1–34, 2015.
- [16] H. Berestycki, B. Nicolaenko, and B. Scheurer. Traveling wave solutions to combustion models and their singular limits. *SIAM Journal on Mathematical Analysis*, 16(6), 1985.
- [17] H. Berestycki, S. Nordmann, and L. Rossi. Activity/Susceptibility systems. *to appear*, 2020.
- [18] H. Berestycki and N. Rodríguez. Analysis of a heterogeneous model for riot dynamics: the effect of censorship of information. *European Journal of Applied Mathematics*, 27(3):554–582, jun 2016.
- [19] H. Berestycki, N. Rodríguez, and L. Ryzhik. Traveling Wave Solutions in a Reaction-Diffusion Model for Criminal Activity. *SIAM Journal on Multiscale Modeling and Simulation*, 11(4), 2013.
- [20] H. Berestycki, L. Rossi, and N. Rodríguez. Periodic cycles of social outbursts of activity. *Journal of Differential Equations*, 264(1):163–196, jan 2018.
- [21] S. Bhattacharya, K. Gaurav, and S. Ghosh. Viral marketing on social networks: An epidemiological perspective. *Physica A*, 525:478–490, 2019.
- [22] L. Bonnasse-Gahot, H. Berestycki, M.-A. Depuiset, M. B. Gordon, S. Roché, N. Rodriguez, and J.-P. Nadal. Epidemiological modelling of the 2005 French riots: a spreading wave and the role of contagion. *Scientific Reports*, 8(1):107, dec 2018.
- [23] J.-P. Bouchaud. Crises and Collective Socio-Economic Phenomena: Simple Models and Challenges. *Journal of Statistical Physics*, 151(3-4):567–606, may 2013.
- [24] D. Braha. Global Civil Unrest: Contagion, Self-Organization, and Prediction. *PLoS ONE*, 7(10):1–9, 2012.
- [25] S. L. Burbeck, W. J. Raine, and M. J. Stark. The dynamics of riot growth: An epidemiological approach. *The Journal of Mathematical Sociology*, 6(1):1–22, 1978.
- [26] B. Cao, S.-H. Han, and Z. Jin. Modeling of knowledge transmission by considering the level of forgetfulness in complex networks. *Physica A*, 451:277–287, 2016.
- [27] P. Caroca, C. Cartes, T. P. Davies, J. Olivari, S. Rica, and K. Vogt. The anatomy of the 2019 Chilean social unrest. *arXiv preprint*, 2020.
- [28] T. P. Davies, H. M. Fry, A. G. Wilson, and S. R. Bishop. A mathematical model of the London riots and their policing. *Scientific Reports*, 3, 2013.
- [29] K. Dietz. Epidemics and Rumours: A Survey. *Journal of the Royal Statistical Society. Series A (General)*, 130(4):505–528, 1967.
- [30] R. Ducasse and L. Rossi. Blocking and invasion for reaction-diffusion equations in periodic media. *ArXiv preprint*, 2018.
- [31] M. Edmonds. *How Riots Work*, 2011.
- [32] J. M. Epstein. Modeling civil violence: An agent-based computational approach. *Proceedings of the National Academy of Sciences*, 99(Supplement 3):7243–7250, may 2002.
- [33] G. Fibich. Bass-SIR model for diffusion of new products in social networks. *Physical Review E*, 94:32305, 2016.
- [34] G. Fibich. Diffusion of new products with recovering consumers. *Society for Industrial and Applied Mathematics*, 77(4):1230–1247, 2017.

- [35] M. Fonoberova, V. A. Fonoberov, I. Mezic, J. Mezic, P. J. Brantingham, A. Societies, and S. Simulation. Nonlinear Dynamics of Crime and Violence in Urban Settings An Agent-Based Model of Civil Violence. *Journal of Artificial Societies and Social Simulation*, 15(2):1–15, 2012.
- [36] J. T. Gardner. A Sensitivity Analysis of an Epidemiological Model of Viral Marketing: When Viral Marketing Efforts Fall Flat. Technical report, 2013.
- [37] N. Gaumont, M. Panahi, and D. Chavalarias. Reconstruction of the socio-semantic dynamics of political activist Twitter networks—Method and application to the 2017 French presidential election. *PLOS ONE*, 13(9), sep 2018.
- [38] S. Gavrillets. Collective action problem in heterogeneous groups. *Philosophical Transactions of the Royal Society B: Biological Sciences*, 370(1683), dec 2015.
- [39] W. Goffman, V. A. Vaun, and A. Newill. Generalization Of Epidemic Theory An Application To The Transmission Of Ideas. *Nature*, 4955, 1964.
- [40] J. N. C. Gonçalves, H. S. Rodrigues, and M. T. T. Monteiro. A Contribution of Dynamical Systems Theory and Epidemiological Modeling to a Viral Marketing Campaign. In *Intelligent Systems Design and Applications*, pages 974–983. Springer, Cham, dec 2017.
- [41] M. B. Gordon, J.-P. Nadal, D. Phan, and V. Semeshenko. Discrete choices under social influence: generic properties. *Mathematical Models and Methods in Applied Sciences*, 19(supp01):1441–1481, aug 2009.
- [42] M. Granovetter. Threshold Models of Collective Behavior. *American Journal of Sociology*, 83(6):1420–1443, may 1978.
- [43] N. Gurley and D. K. Johnson. Viral economics: an epidemiological model of knowledge diffusion in economics. *Oxford Economic Papers*, 69(1):320–331, jan 2017.
- [44] H. Hethcote. The Mathematics of Infectious Diseases. *SIAM Review*, 42(4):599–653, 2000.
- [45] H. W. Hethcote. Three Basic Epidemiological Models. In S. Levin, T. Hallam, and L. Gross, editors, *Applied Mathematical Ecology. Biomathematics, vol 18*, pages 119–144. Springer, Berlin, Heidelberg, 1989.
- [46] F. C. Hoppensteadt. *Mathematical methods of population biology*. Cambridge University Press, Cambridge, 1982.
- [47] R. A. Jeffs, J. Hayward, P. A. Roach, and J. Wyburn. Activist Model of Political Party Growth. *Physica A: Statistical Mechanics and its Applications*, 442:359–372, 2016.
- [48] D. I. Kaiser, M. A. Bettencourt, A. Cintro, and C. Castillo-cha. The power of a good idea: Quantitative modeling of the spread of ideas from epidemiological models. *Physica A: Statistical Mechanics and its Applications*, 364:513–536, 2006.
- [49] K. Kawachi. Deterministic models for rumor transmission. *Nonlinear Analysis: Real World Applications*, 9:1989–2028, 2008.
- [50] W. Kermack and A. McKendrick. A contribution to the Mathematical Theory Of Epidemics. *Proceedings of the Royal Society A*, 115(772), 1927.
- [51] I. Z. Kiss, M. Broom, P. G. Craze, and I. Rafols. Can epidemic models describe the diffusion of topics across disciplines? *Journal of Informetrics*, 4:74–82, 2010.
- [52] J. Lang and H. De Sterck. The Arab Spring: A simple compartmental model for the dynamics of a revolution. *Mathematical Social Sciences*, 69:12–21, may 2014.
- [53] M. Lewis, S. V. Petrovskii, and J. Potts. *The Mathematics Behind Biological Invasions*. Springer International Publishing, 2016.
- [54] Q. Liu, T. Li, and M. Sun. The analysis of an SEIR rumor propagation model on heterogeneous network. *Physica A*, 469:372–380, 2017.

- [55] M. Lynch. *The Arab uprising : the unfinished revolutions of the new Middle East*. PublicAffairs, 2013.
- [56] H. MacGregor, M. Leach, A. Wilkinson, and M. Parker. COVID-19 – a social phenomenon requiring diverse expertise, apr 2020.
- [57] V. Mendez, S. Fedotov, and H. Werner. *Reaction-Transport Systems*. Springer-Verlag Berlin Heidelberg, 2010.
- [58] J. Miller. Mathematical models of SIR disease spread with combined non-sexual and sexual transmission routes. *Infectious Disease Modelling*, 2:section 2.1.3, 2017.
- [59] D. Mistry, Q. Zhang, N. Perra, and A. Baronchelli. Committed activists and the reshaping of status-quo social consensus. *Physical Review E - Statistical, Nonlinear, and Soft Matter Physics*, 92(4), oct 2015.
- [60] D. Moritz Marutschke and H. Ogawa. Clustering Scientific Publication Trends in Cultural Context Using Epidemiological Model Parameters. *Procedia Technology*, 18:90–95, 2014.
- [61] A. Morozov, S. Petrovskii, and S. Gavrilets. The Yellow Vests Movement - a case of long transient dynamics ? *SocArXiv*, pages 1–20, 2019.
- [62] E. N. Nepomuceno, D. F. Resende, and M. J. Lacerda. A Survey of the Individual-Based Model applied in Biomedical and Epidemiology Research. *Journal of Biomedical Research and Reviews*, 1(1):1–11, 2018.
- [63] M. Perrie. The Russian Peasant Movement of 1905-1907: Its Social Composition and Revolutionary Significance. *The Past and Present Society*, 57:123–155, 2020.
- [64] S. Petrovskii, W. Alharbi, A. Alhomairi, and A. Morozov. Modelling Population Dynamics of Social Protests in Time and Space : The Reaction-Diffusion Approach. *Mathematics*, 8(1), 2020.
- [65] Z. Qian, S. Tang, X. Zhang, and Z. Zheng. The independent spreaders involved SIR Rumor model in complex networks. *Physica A*, 429:95–102, 2015.
- [66] R. M. Raafat, N. Chater, and C. Frith. Herding in humans. *Trends in Cognitive Sciences*, 13(10):420–428, 2009.
- [67] H. S. Rodrigues and M. Fonseca. Viral marketing as epidemiological model. In *Proceedings of the 15th International Conference on Computational and Mathematical Methods in Science and Engineering, CMMSE*, number July, 2015.
- [68] S. Ruan. Spatial-Temporal Dynamics in Nonlocal Epidemiological Models. In *Mathematics for Life Science and Medicine*, pages 97–122. Springer, 2007.
- [69] F. J. Santonja, A. C. Tarazona, and R. J. Villanueva. A mathematical model of the pressure of an extreme ideology on a society. *Computers & Mathematics with Applications*, 56:836–846, 2008.
- [70] A. Schussman and S. A. Soule. Process and Protest: Accounting for Individual Protest Participation. *Social Forces*, 84(2):1083–1108, 2005.
- [71] C. I. Siettos and L. Russo. Mathematical modeling of infectious disease dynamics. *Virulence*, 4(4):295–306, may 2013.
- [72] J. Skaza and B. Blais. Modeling the infectiousness of Twitter hashtags. *Physica A*, 465:289–296, 2017.
- [73] L. M. Smith, A. L. Bertozzi, P. J. Brantingham, G. E. Tita, and M. Valasik. Adaptation of an ecological territorial model to street gang spatial patterns in los angeles. *Discrete and Continuous Dynamical Systems*, 32(9):3223–3244, 2012.
- [74] D. A. Snow, R. Vliegthart, and C. Corrigan-Brown. Framing the French Riots: A Comparative Study of Frame Variation. *Social Forces*, 86:385–415, 2007.

- [75] M. J. A. Stark, W. J. Raine, S. L. Burbeck, and K. K. Davison. Some Empirical Patterns in a Riot Process. *American Sociological Review*, 39(6):865–876, 1974.
- [76] P. C. V. On Nonlinear Reaction-Diffusion Systems. *Journal of Mathematical Analysis and Applications*1, 87(1), 982.
- [77] E. Vynnycky and R. G. White. *An introduction to infectious disease modelling*. Oxford University Press, Oxford, 2010.
- [78] J. Wang, L. Zhao, and R. Huang. SIRaRu rumor spreading model in complex networks. *Physica A*, 398:43–55, 2014.
- [79] L. Wang and B. C. Wood. An epidemiological approach to model the viral propagation of memes. *Applied Mathematical Modelling*, 35(11):5442–5447, 2011.
- [80] Wikipedia. Mouvement des Gilets jaunes.
- [81] J. Woo and H. Chen. Epidemic model for information diffusion in web forums: experiments in marketing exchange and political dialog. *SpringerPlus*, 5(1):66, dec 2016.
- [82] C. Yang and N. Rodriguez. A numerical perspective on traveling wave solutions in a system for rioting activity. *Applied Mathematics and Computation*, 364, jan 2020.
- [83] P. A. Yurevich, M. A. Olegovich, S. V. Mikhailovich, and P. Y. Vasilievich. Modeling conflict in a social system using diffusion equations. *SIMULATION*, 94(12):1053–1061, dec 2018.
- [84] Y. Zan, J. Wu, P. Li, and Q. Yu. SICR rumor spreading model in complex networks: Counterattack and self-resistance. *Physica A*, 405:159–170, 2014.
- [85] L. Zhao, J. Wang, Y. Chen, Q. Wang, J. Cheng, and H. Cui. SIHR rumor spreading model in social networks. *Physica A*, 391:2444–2453, 2012.
- [86] L. Zhao, Q. Wang, J. Cheng, Y. Chen, J. Wang, and W. Huang. Rumor spreading model with consideration of forgetting mechanism: A case of online blogging LiveJournal. *Physica A*, 390:2619–2625, 2011.